FLY ASH STABILIZATION OF GRAVEL ROAD AS BASE FOR PAVEMENT AT CHISAGO COUNTY ROAD 53, MINNESOTA

by

Bulent Hatipoglu, Tuncer B. Edil, Craig H. Benson

Geo Engineering Report No. 06-19

Department of Civil and Environmental Engineering
University of Wisconsin-Madison
Madison, Wisconsin 53706
USA

September 19, 2006

EXECUTIVE SUMMARY

This report describes a field site where cementitious fly ashes (Class C and off-specification) were used to stabilize road-surface gravel (RSG) to form a base during construction of a flexible pavement in Chisago County, MN. The project involved conversion of a gravel road to a paved road. It consisted of mixing fly ash (10% by dry weight) and water into the gravel surface to a depth of 254 mm and compacting the mixture to form a firm base, and placement of an HMA surface. California bearing ratio (CBR), resilient modulus (M_r), and unconfined compression (q_u) tests were conducted on a composite sample of the RSG alone and the fly-ash stabilized RSG (S-RSG) samples prepared in the field and laboratory to evaluate how addition of fly ash improved the strength and stiffness. *In situ* testing was also conducted on the subgrade and S-RSG with a soil stiffness gauge (SSG), dynamic cone penetrometer (DCP), and falling weight deflectometer (FWD). A pan lysimeter was installed beneath the roadway to monitor the quantity of water percolating from the pavement and the concentration of trace elements in the leachate. Column leach tests were conducted in the laboratory for comparison.

Addition of fly ash improved the stiffness and strength of the RSG significantly. After 7 d of curing, the S-RSG prepared in the laboratory using materials sampled during construction had CBR mostly ranging between 48 and 90, M_r between 96 and 195 MPa, and unconfined compressive strengths between 197 and 812 kPa, whereas the RSG alone had CBR of 24 and M_r of 51 MPa. Moduli obtained from the FWD inversion were compared with those obtained from the resilient modulus tests on field-mix specimens and the moduli computed from the stiffness measured with the SSG. Moduli obtained from the resilient modulus test on field-mix samples are markedly lower than those obtained from November 2005 FWD but comparable to those from May 2006 FWD. SSG gives 50% higher moduli compared to the modulus obtained from the resilient modulus test. November 2005 FWD data appear anomalously high compared

to other data here and elsewhere. Longer-term monitoring is needed to confirm that the modulus of S-RSG will persist after multiple winter seasons. The CBRs of S-RSG mixed in the field were mostly lower than that for S-RSG mixed in the laboratory; however, the opposite was observed for M_r, and for q_u. This is in contrast with previous experience and being explored further. Laboratory freeze-thaw tests indicate 17% drop in resilient modulus of the S-RSG after 5 cycles of freeze-thaw.

Approximately 29.6 m^3 of leachate corresponding to 3,183 mm of total drainage occurred in the lysimeter during the monitoring period from November 2005 to June 2006. This corresponds to 48 pore volumes of flow by June 15, 2006. The low lying topography of the area and the heavy precipitation that occurred in Spring 2006 may have led to flooding of the lysimeter as these are very high numbers. All of the trace element concentrations (with the exception of Mn) are below USEPA maximum contaminant levels (MCLs) and Minnesota health risk levels (HRLs). Most of the concentrations appear to be stabilizing and persistent. Concentrations of some elements appear to be low and decreasing (e.g.,Pb, Sb and Sn). The trace element concentrations in the column leach test (CLT) effluent typically are higher than concentrations in the drainage collected in the field in the lysimeters. The poor agreement suggests that the CLT test method that was used may not be appropriate for evaluating leaching of trace elements from S-RSG, unless a conservative estimate of the trace element concentrations is acceptable. Despite the higher concentrations obtained from the CLT, most of the elements have concentrations below USEPA MCLs and Minnesota HRLs. The exceptions are B, Be, Cr, Ba,As, and Se. Additional study is also needed to define laboratory leach testing protocols that can more accurately simulate leaching of trace elements from S-RSG.

This page left blank intentionally.

ACKNOWLEDGEMENT

This page left blank intentionally.

TABLE OF CONTENTS

This page left blank intentionally.

LIST OF TABLES

LIST OF FIGURES

This page left blank intentionally.

1.   INTRODUCTION

Utilization of byproducts is becoming a common method to improve the ride quality and structural capacity of roads. Use of self-cementitious fly ash in stabilizing the existing road-surface gravel to form a stable base for hot mixed asphalt layer was implemented in the conversion of a gravel road (CR 53) to a paved road in Chisago County, MN.

A study was conducted to evaluate both short and long term geo-mechanical and geo-environmental performance of the road constructed using fly ash stabilization by UW-Madison Geo Engineering Program.   In the framework of the study resilient modulus, California Bearing Ratio (CBR), unconfined compressive strength, soil stiffness gauge (SSG), dynamic cone penetrometer (DCP), falling weight deflectometer (FWD) tests have been performed to evaluate the geo-mechanical characteristics. DCP and SSG were performed on both subgrade and stabilized base. Resilient modulus, CBR and unconfined compressive strength tests were conducted on fly ash mixed in the field prepared right after construction an cured for 7 days. A lysimeter was constructed for assessing ground water impacts associated with leaching of metals from fly-ash stabilized subgrade. Column leaching tests were performed to asses the leaching characteristics of fly ash stabilized road-surface gravel. An automated field monitoring system was installed to observe the climatic conditions and provide a basis to interpret the geo-mechanical and geo-environmental performance of the roadway.   The field instrumentation measures and records air temperature, relative humidity and precipitation. Volumetric water content and temperature in base, subbase, and subgrade at six locations.

This report describes a project where self-cementing fly ashes from a coal-fired electric power plant were used to stabilize an existing gravel road to form a base for

HMA pavement during reconstruction as a paved road of a 3.6-km section of gravel County Road 53 in Chisago County, MN ($\approx$ 88 km north of Saint Paul, MN). The area where fly ash stabilized material placed was cut and shaped in conformance with the lines and grades given on the plans. Then cementitious fly ash (10% by dry weight) was spread uniformly on the surface using truck-mounted lay-down equipment similar to that described in Edil et al. (2002). The fly ash was mixed with a CMI RS-650-2 road reclaimer into the gravel road to a depth of 254 mm, with water being added during mixing using a water truck (see photographs in Appendix A). This mixture, which contained 10% fly ash by dry weight, was compacted within 1-2 hr by a tamping foot compactor followed by a vibratory steel drum compactor. The S-RSG was overlain with 51 mm non-wearing course and 38 mm wearing course (total 89 mm) of HMA within 3 to 7 days after compaction of the fly ash stabilized base.

## 2.	DESCRIPTION OF THE SITE AND CONSTRUCTION

2.1. Site Description

Chisago County Road 53 (CR 53) is located at the 88 km north of the Saint Paul, MN runs north-south parallel to and west of I-35.   The field study was conducted between stations 0+00 to 104+00 of CR 53 (Fig. 1). Road surface had not been covered by pavement and consisted of gravelly clayey sand before the construction.   The purpose of the new construction work was to increase the strength of the road-surface gravel to form a base for the new asphalt pavement.

CR 53 lies on a flat topography in this area formed in Pine City ground moraine (primarily classified as lean clay). Twenty one borings (Appendix B) were performed along the length of the construction site that indicated presence of approximately 0.6-m thick sandy gravel fill forming the pavement structure. The gravel fill was underlain mostly by lean clay and occasionally poorly graded sand. The thickness of the gravel fill was less than 0.3-m when sand subgrade was encountered. Groundwater level is about 1 m below the existing gravel road.

2.2. Construction

Fly ash was spread uniformly in strips directly over the gravel road until the width of the whole road cross section was covered. The fly ash was spread by special truck-mounted lay-down equipment (Fig. 2a). Top 254 mm of working platform was mixed with fly ash using a CMI RS-650-2 road reclaimer. During the mixing process, water was added from a water tanker truck attached to the reclaimer to provide optimum water content. Immediately after the mixing process, a sheep foot compactor and a vibratory compactor with steel drum were used to compact the mixture in sequence to complete

3

the stabilization process (Fig. 2b). Compaction was completed within 1 to 2h after mixing. The mixed material was compacted to a target relative compaction of 95% based on standard Proctor energy (ASTM D 698). The standard Proctor maximum dry unit weight was 21.9 kN/m^3 and the optimum water content of 6%. Working platform stabilized with fly ash was stiff and ready to be covered by asphalt concrete pavement. Construction started on August 23, 2005 and ended on August 26, 2005. The bituminous non wear course was paved on September 8, 2005 and the bituminous wear course was paved on September 9, 2005.

3.   MATERIALS

3.1 Subgrade

In order to characterize the engineering properties of soil profile, ten sampling points were selected at construction stations of 10+00, 20+00, 27+30, 40+00, 50+00, 60+00, 70+00, 80+30, 90+00 and 104+00 in the middle of east bound lane. Disturbed samples of subgrade soil and road-surface gravel (RSG) ($\approx$ 20 kg each) were collected at these 10 stations during construction (see the construction route from Station 0+00 to 115+00 in Fig. 1). A backhoe was used to obtain samples of RSG and expose the subgrade. On the exposed subgrade surface, in situ water content and dry unit weight were measured using a nuclear gauge, a stiffness measurement was made using the Soil Stiffness Gauge (SSG), and a dynamic penetration index (DPI) was determined using a Dynamic Cone Penetrometer (DCP) .   The data obtained are given in Table 1 along with estimated California Bearing Ratio (CBR) and elastic modulus corresponding to weighted DPI over a depth of about 150 mm.   CBR was estimated from the relationship given by the US Army Corps of Engineers as follows

$$CBR = 292 * DPI^{-1.12} \tag{1}$$

where CBR in percent, DPI in mm per blow. Elastic modulus was estimated from CBR using a well known UK Transportation Research Laboratory equation (Powell et al. 1984) as follows

$$E = 17.6 * CBR^{0.64} \tag{2}$$

where E is in MPa and CBR is in percent.

CBR of the subgrade soils ranges from 5 to 33 (mean = 14). Stations 20+00, 40+00 and 50+00 had CBR of 5-7 classifying as fair subgrade, all other stations had a CBR of 8

or more classifying as a medium to good subgrade. The elastic modulus of the subgrade ranges from 48 to 165 MPa (mean = 90 MPa). These values are reflective of the low water content of the subgrade at the time these measurements were made.

Subgrade samples were visually classified and grouped into five groups. Samples in each group were mixed together to create five composite samples and Atterberg limits and grain size distribution tests were performed on the composites. The Atterberg limits and percent fines are given in Table 2 along with group index and AASTHO and USCS classifications.   The grain size distribution of each composite group is given in Fig. 3. The subgrade consists of silty sands (SM and SP-SM) or sandy low plasticity clays (CL and CL-ML) according to the Unified Soil Classification System. According to the AASHTO Soil Classification System, most subgrade soils at this site are A-2-4 with a group index (GI) of 0. Other subgrade soils classify as A-3, A-4, and A-5.

3.2 Road-surface gravel (RSG)

A summary of the textural characteristics of the RSG is shown in Table 3 and grain size distribution curves for the RSG are shown in Fig. 4. The grain size distribution curves fall in a relatively narrow band. The RSG samples consist of well-graded gravelly sand with fines in the range of 11 to 14% except Station 90+00 where fines content is 22%. The sand content is consistently around 60% and the gravel content is about 25%. Because of the very similar nature of the RSG along the construction route, a composite sample was prepared for conducting laboratory tests. It is classified as gravelly clayey sand according to Unified Soil Classification system (ASTM D2487).

Compaction tests were performed on a sample from Station 27+30 (near the pan lysimeter location, Fig.1.)   and on the composite sample as shown in Fig. 5. The

optimum water content is approximately 9% and the maximum dry unit weight is 20 kN/m^3 for both samples based on standard compaction effort. The effect of grains larger than #4 sieve on compaction is observable in Fig. 5b. (the optimum moisture content is lowered by 1% and the unit weight is increased by 1.4 kN/m^3). The compaction test performed by GME Consultants, Inc for Chisago County prior to construction indicated an optimum water content of approximately 6% and a maximum dry unit weight of 21.9 kN/m^3 based on standard compaction effort (ASTM D 698).

3.2 Fly Ash

Fly ashes from Riverside Unit 7 and Riverside Unit 8 power station at Saint Paul, MN were used for stabilization. Table 4 shows the types of fly ashes used in each station location. Chemical composition and physical properties of the fly ashes are given in Table 5 along with the composition of typical Class C and F fly ashes as well as the ASTM and AASHTO specifications for class C fly ash. Calcium oxide (CaO) contents of Riverside 7 and Riverside 8 fly ashes are 24% and 22% and silicon oxide (SiO$_2$) contents are 32% and 19% respectively. CaO/SiO$_2$ ratios, which are indicative of cementing potential are 0.75 and 1.18. Loss of ignition (LOI), which is the indication of the amount of unburned coal in the fly ash are 0.9% and 16.4%, respectively. According to ASTM C 618, Unit 7 fly ash is a Class C fly ash whereas Unit 8 fly ash is an off-specification self-cementing fly ash. In this project, 10% fly ash by weight was mixed with RSG.

3.3 Stabilized Road-surface gravel (S-RSG)

Water content and unit weight of the compacted S-RSG were measured at each station using a nuclear density gage (ASTM D 2922) immediately after compaction was

completed. Grab samples ($\approx$ 20 kg) of S-RSG were also collected at these locations and were compacted in the field into a CBR mold (114 mm inside diameter x 152 mm height) and a resilient modulus mold (102 mm inside diameter x 203 mm height) to the unit weight measured with the nuclear density gage. Three lifts were used for the CBR specimens and six lifts were used for the M_r specimens. After compaction, the specimens were sealed in plastic and stored at 100% humidity for curing for approximately 7 days. These test specimens are referred to henceforth as 'field-mix' specimens. Because of the cementing effects of the fly ash, index testing was not conducted on the S-RSG.

Specimens of S-RSG were also prepared in the laboratory using the composite sample prepared by mixing samples of RSG collected during construction with River Side Unit 8 fly ash. These specimens, referred to henceforth as 'laboratory-mix' composite specimens, were prepared with 10% fly ash (dry weight) at the mean field water content (6.4%) and mean dry unit weight (19.3 kN/m^3). The laboratory-mix specimens were compacted and cured using the procedures employed for the field-mix specimens. Similarly a specimen was prepared with the composite RSG only (no fly ash) at a dry unit weight of 19.3 kN/m^3 in an air-dry condition.

4.   LABORATORY TEST METHODS

4.1 CBR

The CBR tests were conducted in accordance with ASTM D 1883 after 7 d of curing (field-mix or laboratory-mix S-RSG) or immediately after compaction (RSG). The specimens were not soaked and were tested at a strain rate of 1.3 mm/min. The 7-d curing period and the absence of soaking are intended to represent the competency of the RSG when the HMA is placed (Bin-Shafique et al., 2004). Data from the unsoaked CBR tests were not intend as a measure of stiffness of the S-RSG and are not for use in pavement design with S-RSG.

4.2 Resilient Modulus and Unconfined Compression Tests

Resilient modulus tests on the S-RSG and RSG were conducted following the methods described in AASHTO T292 after approximately 7 d of curing (S-RSG) immediately after compaction (RSG). Turner (1997) recommended a 14-d curing period, intended to reflect the condition when most of the hydration is complete (Edil et al., 2006). However, here only 7 days of curing was employed to compare with the field measurements done after a similar period. The loading sequence for cohesive soils was used for the S-RSG as recommended by Bin-Shafique et al. (2004) and Trzebiatowski et al. (2004) for soil-fly ash mixtures. RSG was tested using the loading sequence for cohesionless soils. Unconfined compressive strength was measured on specimens of S-RSG after the resilient modulus tests were conducted. A strain rate of 0.21%/min was used for the unconfined compression tests following the recommendations in ASTM D 5102 for compacted soil-lime mixtures. No standard method currently exists for unconfined compression testing of materials stabilized with fly ash, including stabilized RSG.

Freeze-thaw effects were also investigated in the laboratory through resilient modulus and post-resilient modulus unconfined compression tests performed on composite RSG specimens stabilized with 10% Riverside 8 fly ash identically prepared and cured as described earlier. Four specimens were prepared in replicate. One set was tested immediately following the curing process. The remaining three sets were subjected to 1, 3, and 5 cycles of freeze and thaw and then tested. The procedure of freeze-thaw cycling is described by Rosa (2006). Her tests on a variety of fly ash stabilized and unstabilized materials showed that the freeze-thaw effects stabilize after 5 cycles, thus 5 cycles were applied. A freezing-point depression test following ASTM 5918 was performed on the RSG and S-RSG to determine the temperature at which freeze the specimens. The freezing-point depression was 11 and 12 ^{o}C for RSG and S-RSG, respectively; so the specimens were frozen to 15 ^{o}C three-dimensionally during the freeze-thaw cycles. ASTM D 6035 was used as a guide for this procedure. This standard describes a method to determine the freeze-thaw effects on hydraulic conductivity. Specimens prepared for freeze-thaw cycles had a thermocouple embedded in the third layer. After curing, specimens were extruded from the molds. After extrusion from PVC molds, the specimens were soaked for five hours. The specimens were then wrapped in plastic to prevent changes in moisture content during freeze-thaw cycling and placed in a freezer to begin cycling. The embedded thermocouples were used to confirm freezing. Thawing took place at room temperature.

4.3 Column Leaching Test

Column leach tests (CLT) were conducted on samples of field-mix S-RSG collected from Stations 2 and 5 (20+00 and 40+00). The specimens were prepared in the field in a standard Proctor compaction mold (height = 116 mm, diameter = 102 mm)

using the same procedure employed for the specimens of field-mix S-RSG prepared for CBR testing. The specimens were cured for 7-d prior to testing.

The CLT was conducted following the procedure described in ASTM D 4874, except a flexible-wall permeameter was used instead of a rigid-wall permeameter as shown in Fig. 6. Flow was oriented upward and was driven by a peristaltic pump set to provide a Darcy velocity of 2 mm/d. The effective confining pressure was set at 15 kPa. A 0.1 M LiBr solution was used as the permeant liquid to simulate percolate in regions where salt is used to manage ice and snow (Bin-Shafique et al. 2006). Effluent from the column was collected in sealed Teflon bags to prevent interaction with the atmosphere. Leachate was removed from the bags periodically ($\approx$ 30 ~ 60 mL of flow accumulation). Volume of the leachate removed was measured, the pH was recorded, and a sample was prepared for chemical analysis by filtering with a 0.45 μm filter and preservation with nitric acid to pH < 2.

All effluent samples were analyzed by inductively coupled plasma-mass spectrometry (ICP-MS) following the procedure described in USEPA Method 200.8. Analysis was conducted for the following elements (detection limits in μg/L in parentheses): Ag (0.02), As (0.1), B (0.2), Ba (0.02), Be (0.02), Ca (5), Cd (0.08), Co (0.01), Cr (0.04), Cu (0.07), Hg (0.2), Mo (0.08), Mn (0.03), Ni (0.05), Pb (0.01), Sb (0.02), Se (2.0), Sn (0.04), Sr (0.01), Tl (0.006), V (0.06), and Zn (0.2).

5. FIELD METHODS

5.1 Environmental Monitoring

The environmental monitoring program consists of monitoring the volume of water draining from the pavement, concentrations of trace elements in the leachate, temperatures and water contents within the pavement profile, and meteorological conditions (air temperature, humidity, and precipitation). Monitoring of the pavement began in November 2004 and is still being conducted.

Leachate draining from the pavement was monitored using a pan lysimeter installed at Station 27+30 (Fig. 1). The test specimens for the CLT (Section 4.3) were collected at Stations 2 and 5 (20+00 and 40+00) on either side of the pan lysimeter location, so that a comparison could be made between leaching measured in the field and laboratory. The lysimeter is 4 m wide, 4 m long, and 200 mm deep and is lined with 1.5-mm-thick linear low density polyethylene geomembrane. The base of the lysimeter was overlain by a geocomposite drainage layer (geonet sandwiched between two non-woven geotextiles). S-RSG was placed in the lysimeter and compacted using the same method employed when compacting S-RSG in other portions of the project. Photographs showing the lysimeter construction are in Fig. 7.

Water collected in the drainage layer is directed to a sump plumbed to a 120-L polyethylene collection tank buried adjacent to the roadway. The collection tank is insulated with extruded polystyrene to prevent freezing. Leachate that accumulates in the collection tank is removed periodically with a pump. The volume of leachate removed is recorded with a flow meter, a sample for chemical analysis is collected, and the pH and Eh of the leachate are recorded. The sample is filtered, preserved, and analyzed using the same procedures employed for the CLT (Section 4.3). Personnel from the Chisago County collected the samples from the lysimeter.

Conditions in the fly ash stabilized subbase and subgrade are being monitored continuously at station 27+30. The data being collected include air temperature and relative humidity; subsurface temperature and volumetric water content; quantity and quality of water percolating from the fly ash stabilized subbase layer into the pan lysimeter. Air temperature and relative humidity (RH) are measured with a thermistor and a capacitive relative humidity sensor (Fig. 8). The Campbell Scientific Inc. (CSI) HMP35C temperature/RH probe is housed in a radiation shield to eliminate the effects of solar radiation (Figure 8b). A Rain gage (CSI TE 525) is used to measure precipitation.

Subsurface volumetric water contents in the S-RSG and the subgrade soils are measured using CSI CS616 water content reflectometers (WCRs). Two of WCRs installed in the S-RSG layer at 216 and 241 mm depths from the pavement surface. The other two WCRs were placed in the subgrade soil at depths 445 and 700 mm from the pavement surface. Locations of the WCRs are shown in Fig. 8a. WCRs employ a time-domain reflectometry (TDR) methodology that relates the round-trip travel time of an electromagnetic pulse along a wave to the volumetric water content of the medium in which it is placed. The travel time is function of the dielectric content of the soil or S-RSG, which is strongly influenced by water content (Benson and Bosscher, 1999). Material-specific calibration curves are required to obtain accurate volumetric water contents.

Subsurface temperature is measured at 6 locations in the S-RSG and the subgrade using Type-T copper-constantan thermocouples. Thermo couples were wired to datalogger trough an AM25T type multiplexer. Locations of the duplex insulated thermocouples are shown in Fig. 8a.

Data from the meteorological and subsurface sensors are collected with a CSI CR 23X datalogger powered by a 12-V deep-cycle battery and a solar panel. Data are

13

downloaded from the datalogger via telephone modem.   Photograph of the instrumentation are included in Fig. 8b.

5.2 Mechanical Evaluation of Pavement Materials

Strength and stiffness of the S-RSG were measured with a soil stiffness gauge (SSG), a dynamic cone penetrometer (DCP), and a falling weight deflectometer (FWD). Photographs of the testing are included in Appendix A. Testing with the SSG and DCP, was conducted directly on the S-RSG after approximately 7 d of curing. FWD testing was conducted two times after the HMA was placed (November 8, 2005 and May 9, 2006).

The SSG tests were conducted in accordance with ASTM D 6758 using a Humboldt GeoGauge. Two or three measurements were made at each station within a 0.1-m radius. These measurements deviated by less than 10%. Thus, the mean of these stiffness measurements is reported herein. DCP testing was conducted at each station in accordance with ASTM D 6951 using a DCP manufactured by Kessler Soils Engineering Products Inc. The dynamic penetration index (DPI) obtained from the DCP was computed as the weighted penetration (mm per blow) over a depth of 150 mm.

FWD tests were conducted at each station by Braun Intertec Inc. in November 2005 (2 months after construction) and in May 2006 (one year after construction) using a Dynatest^{TM} 8002E FWD following the method described in ASTM D 4694. Moduli were obtained from the FWD deflection data by inversion using MODULUS 6.0 from the Texas Transportation Institute. Analysis of the FWD data was conducted at the University of Wisconsin-Madison.

6.   ENVIRONMENTAL DATA

6.1. Meteorological and Subsurface Conditions

Air temperature and relative humidity between November 2005 and May 2006 are shown in Fig. 9.   The air temperature ranged from -27 and 34 ^{o}C during the monitoring period, with sub-freezing temperatures occurring between November and April.

Precipitation record at the site was obtained from the nearest weather station at Cambridge, MN. The cumulative precipitation is shown in Fig. 10 for the period from November 2005 to May 2006.

The air temperature and the subsurface temperatures and the volumetric water contents as measured by sensors 1, 2, 3, and 4 (see Fig. 8a) are plotted in Figs. 11 trough 14.   Additional subsurface temperatures were measured by sensors 5 and 6 at depths of 241 and 685 mm, respectively.   They are plotted along with the air temperature in Fig. 15 for the period October 2005 to April 2006.   Temperature of the S-RSG (Sensors 3 and 4) ranged between -10 ^{o}C and 35 ^{o}C (Figs. 11 and 12).   This layer was frozen for about 3-4 months.   The temprature of the unstabilized RSG ranged between -1 or -4 ^{o}C and 31 ^{o}C   (Figs. 13 and 15).   This layer also experienced subfreezing temperatures for about 3-4 months but the temperature was slightly below the freezing point.   Furthermore, subfreezing temperatures penetrated for very short periods after major cold air temperature spells in December and February.   The subsurface temperatures varied seasonally with the air temperature.   The magnitude and frequency of variation diminishes with depth, which reflects the thermal damping provided by the pavement materials.   Overall, the main layer that experienced freezing was the S-RSG although some penetration occurred below this layer.   Main frost effects on the pavement would be expected to emanate from this layer.

The volumetric water contents are given in Figs. 11 and 12 for the S-RSG layer, in Fig. 13 for the RSG layer, and Fig. 14 for the subgrade. The volumetric water contents drop when the soil temperature begins to fall below 0 $^{\circ}$C (volumetric water contents are not reported in these figures for periods when freezing was established). These apparent drops in water content reflect freezing of the pore water. The water content measured by WCRs is determined by measuring the velocity of an electromagnetic wave propagated along the probe. The velocity of the wave varies with the apparent dielectric constant of the soil, which is dominated by the dielectric constant of the water phase. When the pore water freezes, the dielectric constant of the water phase drops significantly, which appears as a drop in water content in WCR data (Benson and Bosscher 1999).

Higher volumetric water contents were recorded in the fine-textured subgrade (maximum of about 33.5%) than the coarse-grained RSG (maximum of 28%), which reflects the greater propensity of fine-textured soils to retain water. The volumetric water content of SRGS, however, was quite high (up to 44 to 54%). This may be partly due to calibration as we have not yet obtained the calibration curves for S-RSG but used the curves for SRPM from Waseca project. This will be revised. No spikes are present in the water content records, which reflects the ability of the HMA to impede infiltration during precipitation and snow melt events and to limit evaporation during drier periods. The annual variation in water content is relatively small in the subgrade and the RSG layer, with a larger variation in the S-RSG layer. Higher water contents are recorded in the spring, when greater precipitation occurs.

The seasonal variation in water content is also reflected in the drainage collected in the lysimeter, as shown in Fig. 10 when a significant rise is recorded in April 2006.

There is not complete annual record of drainage drainage yet to make definitive conclusions. A complete summary of the lysimeter data is in Appendix C.

6.2 Trace Elements in Lysimeter Drainage

Approximately 29.6 m^3 of leachate corresponding to 3,183 mm of total drainage occurred during the monitoring period from November 2005 to June 2006 as shown in Fig. 16. This corresponds to 16 pore volumes of flow, PVF through the S-RSG by the end of March 2006. This amount has increased to 48 PVF by June 15, 2006. The low lying topography of the area and the heavy precipitation that occurred in Spring 2006 may have led to flooding of the lysimeter as these are very high numbers. For instance, in the City of Waseca only 1.8 PVF occurred over 20 months in a similar arrangement through a fly ash stabilized recycled pavement material.   During this period, pH of the drainage has been near neutral (6.8 – 7.6) and Eh = 41-342 mV. A summary of the pH and Eh data along with the trace element concentrations is in Appendix C.

Concentrations of trace elements in drainage from the lysimeters are shown in Fig. 17 as a function of PVF. The figure is divided into three parts: high concentration, moderate and persistent, and low and diminishing concentration. Elements not shown in Fig. 17 include those below the detection limit (Be, Ag, Hg, and Tl) and elements not typically associated with health risks (e.g., Ca). All of the concentrations are below USEPA maximum contaminant levels (MCLs) and Minnesota health risk levels (HRLs). The exception is Mn, which had a maximum concentration of 3,682 ug/L and exceeded the Minnesoata HRL of 100 ug/L. However, the Minnesota Department of Health no longer recommends the HRL value and plans exist to increase the HRL to 1,000 to 1,300 ug/L (www.pca.state.mn.us). USEPA does not have a MCL for Mn. Most of the

concentrations appear to be stabilizing and persistent. Concentrations of some elements appear to be low and decreasing (Pb, Sb and Sn).

6.3 Trace Elements in CLT Effluent

Two column tests were performed using material from Station 2 and 5 (20+00 and 40+00). Concentrations of trace elements in the effluent from the CLT on the S-RSG are shown in Figs. 18 and 19, respectively for Stations 2 and 5. Elements are plotted separately in 3 groups depending on their peak concentrations in Figs. 18 and 19: those having peak concentrations exceeding 1 mg/L, those having peak concentrations between 10 and 1,000 μg/L, and those having peak concentrations less than 10 μg/L. A compilation of the data is in Appendix D.

Comparison of Fig. 18 with Fig. 19 indicates that the trace element concentrations are comparable for the two samples obtained at two different stations as the same elements are grouped into the same concentration range in both plots. The only exception is Sr which has a peak concentration slightly over 10 μg/L in Station 5 and slightly lower than 10 μg/L in Station 2 sample. Comparison of Figs. 18 and 19 indicates that the trace element concentrations in the CLT effluent typically are higher than concentrations in the drainage collected in the field (Fig. 17). The poor agreement suggests that the CLT test method that was used may not be appropriate for evaluating leaching of trace elements from S-RSG, unless a conservative estimate of the trace element concentrations is acceptable. Despite the higher concentrations obtained from the CLT, most of the elements have concentrations below USEPA MCLs and Minnesota HRLs. The exceptions are for B (peak = 2,820 μg/L in St. 5, no MCL, HRL = 600 μg/L,), Be (peak = 1 and 0.2 μg/L in St. 5 and St. 2 , MCL = 4 μg/L, HRL = 0.08 μg/L), Cr (peak = 801 and 543 μg/L in St. 5 and St. 2, MCL = 100 μg/L, HRL = 100 μg/L), Ba (peak =

4,460 and 4,490 μg/L in St. 5 and St. 2, MCL, HRL = 2,000 μg/L), As (peak = 50 and 37 μg/L in St. 5 and St. 2 , MCL = 10 μg/L, no HRL), and Se (peak = 45 and 48 μg/L in St. 5 and St. 2 , MCL = 50 μg/L, HRL = 30 μg/L).

       The elution behavior observed in the CLT effluent follows two patterns: (i) first-flush response, where the concentration falls from an initially high value and then remains nearly constant, and (ii) persistent leaching, where the concentration initially increases and then remains relatively constant.

7.   PROPERTIES OF S-RSG AND RSG

7.1 Laboratory Test Data

CBR, M_r, and q_u of the S-RSG and RSG are summarized in Table 6. Tests were conducted on the RSG and laboratory-mix S-RSG using the composite sample created by mixing the RSG samples from all of stations. Tests were conducted on both RSG and S-RSG to determine the benefits of adding fly ash to the mixture in terms of strength and stiffness gain but ultimately to assess these values for S-RSG and compare with traditional base course material.

CBR of the field mix S-RSG is given along the alignment of the project in Fig. 20 supplemented with CBR of the S-RSG estimated from DCP along with the laboratory CBR tests on RSG and S-RSG performed using the composite sample.   There is no systematic variation in CBR of the RSG or S-RSG along the alignment, suggesting that the variability in the CBR is more likely due to heterogeneity in the material rather than systematic variation in site conditions or construction methods. A review of the type of fly ash used, Riverside Unit 7 or 8 (i.e., Class C versus off-specification fly ash) (see Table 4) in each station does not reveal any influence of fly ash. For instance, at Stations 27+30, 60, and 70 only Unit 8 (off-specification fly ash) was used whereas at Station 40 only Unit 7 (Class C fly ash) was used. There is no significant difference in CBR between these stations. After 7 d of curing, the S-RSG prepared in the laboratory using materials sampled during construction had CBR mostly ranging between 48 and 90, M_r between 96 and 195 MPa, and unconfined compressive strengths between 197 and 812 kPa, whereas the RSG alone had CBR of 24 and M_r of 51 MPa. At four stations, CBR of the field mix S-RSG varies between 50 and 80 and compares well with good quality gravel base course but lower than crushed rock base course (Hunt 1986). At three stations CBR of field mix S-RSG is around 80. At one station (Station 50), CBR

is much lower (i.e., 16) but this is not supported by the DCP data at that station. Therefore, it is likely due to some sampling error but not a systematic problem. The CBRs as estimated from the field DCP are mostly comparable to field mix CBR but occasionally higher and in no case lower. The curing period was 7 days both for field mix specimens tested in the laboratory and the DCP in the field. The CBR of the laboratory mix S-RSG was 154 and much higher than any of the S-RSG field specimens or tests. The CBR of the composite RSG sample was 24 and RSG is unqualified as a base course based on this CBR. However, adding fly ash to the RSG increased the CBR appreciably, although the CBR in the field was as much as 66% lower than the CBR of the laboratory-mix S-RSG. This is consistent with the observations made at for stabilized recycled pavement material in the City of Waseca (Li et al. 2006) and fine-grained subgrade stabilization (Bin-Shafique et al. 2004). Bin-Shafique et al. (2004) attribute these differences in CBR to more thorough blending of soil and fly ash in the laboratory compared to the field, resulting in more uniform distribution of cements within the mixture.

The CBR of the subgrade soils were estimated from DCP and given in Table 1 and plotted in Fig. 20. Subgrade CBR vary between 5 and 33 (mean = 14). Stations 20+00, 40+00 and 50+00 had CBR of 5-7 classifying as fair subgrade, all other stations had a CBR of 8 or more classifying as a medium to good subgrade.

Resilient moduli data of field mix S-RSG are shown in Fig. 21. Fig. 21a shows resilient modulus as a function of deviator stress. Resilient modulus does not show much dependence on deviator stress within the test range unlike typical cohesive soils. The resilient moduli along the alignment of the project are shown in Fig. 21b. These M_r correspond to a deviator stress of 21 kPa, which represents typical conditions within the base course of a pavement structure (Tanyu et al. 2003, Trzebiatowski et al. 2004). As

observed for CBR, there is no systematic variation in M_r along the alignment. The field-mix S-RSG had M_r between 96 and 195 MPa (mean = 153 MPa). The mean resilient modulus of field-mix S-RSG is markedly higher than the mean resilient modulus of field-mix recycled pavement materials (153 Mpa versus 78 MPa). It is also higher than the typical resilient modulus of crushed rock aggregate (48 to 103 MPa). Mr of the composite RSG and the laboratory mix S-RSG were measured to be about 51 and 80 kPa at typical pavement stresses (Table 6). Adding fly ash increased the M_r. However, M_r of the field-mix S-RSG was higher (twice as much, on average) than the M_r of the laboratory-mix S-RSG. This is not consistent with all other fly ash sites investigated. The laboratory-mix S-RSG tests are being repeated.

Unconfined compressive strength measured on the resilient modulus specimens after the resilient modulus tests of the S-RSG along the alignment of the project are shown in Fig. 22. Strengths are not reported for RSG because the RSG is essentially non-cohesive and therefore is not amenable to q_u testing. As with CBR and M_r, there is no systematic variation in q_u along the alignment. The field-mix S-RSG had q_u between 197 and 812 kPa (mean = 408 kPa). The laboratory mix S-RSG had a q_u of 183 kPa. q_u of the field-mix S-RSG follows the same trend as M_r in comparison to the laboratory-mix S-RSG i.e., lower. The laboratory-mix S-RSG tests are being repeated

Resilient modulus and unconfined compressive strength of the specimens that were subjected to freeze-thaw cycles were normalized by the resilient modulus and unconfined compressive strength of the specimen that was not subjected to any freeze-thaw cycles to determine the loss of property due to freze-thaw. The results are summarized in Table 7. Resilient modulus dropped by 17% after 5 cycles of freeze-thaw. Rosa (2006) performed freeze-thaw tests on a variety of materials including fine-grained soils alone and stabilized with fly ash. The degree of resilient modulus reduction

varied with the type of material but remained to be no more than 50%. S-RSG appears to show resistance to frost damage in the laboratory.

7.2 Field Test Data

A set of SSG measurements were made immediately after S-RSG was compacted in the field. Another set of SSG as well as a set of DCP measurements were made approximately after 7 to 10 days of curing. In situ stiffness measured with the SSG and dynamic penetration index (DPI) measured with the DCP are shown in Fig. 23 for the subgrade and the S-RSG. Subgrade has DPI vary between 7 and 39 mm/blow (mean = 20.4 mm/blow) whereas S-RSG DPI varies between 2 and 5 mm/blow (mean = 3.4 mm/blow) as shown in Fig. 23a.

As shown in Fig. 23b, subgrade SSG stiffness varies between 8 and 17 MN/mm (mean = 11 MN/mm). SSG stiffness of S-RSG varies between 11 and 22 MN/mm (mean = 16 MN/mm) after compaction. SSG stiffness increased with curing and varies between 17 and 34 MN/mm (mean = 27 MN/mm) after 7 days. The DPI and stiffness of the S-RSG are also less variable than those of the subgrade.

The SSG and DPI statistics for the subgrade and the S-RSG are shown in Fig. 24. In this type of box plot, each box encloses 50% of the data with the median value of the variable displayed as a line. The top and bottom of the box mark the limits of ± 25% of the variable population. The lines extending from the top and bottom of each box mark the minimum and maximum values within the data set that fall within an acceptable range. Any value outside of this range, called an outlier, is displayed as an individual point. The effect of stabilization and curing is evident in Fig. 24.

Maximum deflections from the FWD tests for the 40-kN drop are shown in Fig. 25a for November 2005 several months after construction and when the air and ground temperatures were dipping although there was no frost penetration and for May 2006 when ground temperatures but also the volumetric water contents both in RSG and S-RSG layers were significantly higher compared to November 2005 (see Figs. 11, 12, and 13). The volumetric water content of the subgrade layer was comparable between the two FWD testing dates (see Fig. 14). Maximum deflection, which is measured at the center of the loading plate, is a gross indicator of pavement response to dynamic load. Also given on Fig. 23b are the subgrade and S-RSG SSG surveys. There is a marked increase in deflections in May 2006. The deflections in May 2006 are particularly larger at Stations 60+00 to 80+00. The S-RSG stiffness as measured by SSG shows some variation but does not indicate any weakness around Station 60+00. The subgrade stiffness, however, tends to mimic the variation observed in the FWD maximum deflections. Additional data are needed to make reasonable conclusions.

Elastic moduli of the S-RSG that were obtained by inversion of the FWD data are shown in Fig. 26a. For the inversion, a three-layer profile was assumed that consisted of asphalt (89-mm thick), S-RSG (254-mm thick), and an infinitely thick subgrade. Modulus of the asphalt was allowed to vary between 345 and 11,750 MPa and the Poisson's ratio was set as 0.4. The S-RSG was assumed to have a Poisson's ratio of 0.35 and the modulus was allowed to vary between 70-9400 MPa. The subgrade was assumed to have a Poisson's ratio of 0.35.

The modulus of the S-RSG varies between 513 and 1098 MPa (mean = 741 MPa) in November 2005 and between 74 and 199 MPa (mean = 156 MPa) in May 2006. Most of the S-RSG moduli are 600-700 Mpa in November 2005. In May 2006, S-RSG moduli are 100 to 200 MPa at most stations but it is markedly low at Station 70+00. The subgrade

moduli also are lower in May 2006 in comparison to November 2005 but they appear to be fairly uniform along the roadway.

The statistics of elastic moduli as determined from the FWD test for the S-RSG and the subgrade are shown in Fig. 27 over the length of the construction route indicating the drop for both the S-RSG and the subgrade from November 2005 to May 2006. Additional monitoring is needed to understand the trends and the causes. While there is a dramatic drop in the S-RSG modulus, the median value of 162 MPa in May 2006 is comparable to or slightly higher than that of fly ash stabilized recycled pavement material in the City of Waseca as measured in August 2005 (Lin et al. 2006).

Moduli obtained from the FWD inversion are compared with those obtained from the resilient modulus tests on field-mix specimens and the moduli computed from the stiffness measured with the SSG in Fig. 28. Elastic modulus (E) was computed from the SSG stiffness (K_{SSG}) using (Sawangsuriya et al., 2003):

$$E = \frac{K_{SSG}(1 - \upsilon^2)}{1.77\,R} \qquad\qquad (3)$$

where R is the outside radius of the SSG foot (0.057 m) and υ is Poisson's ratio (assumed to be 0.35). Moduli obtained from the resilient modulus test on field-mix samples are markedly lower than those obtained from November 2005 FWD but comparable to those from May 2006 FWD. SSG gives 50% higher moduli than the moduli obtained from the resilient modulus test. November 2005 FWD data appear anomalously high compared to other data here and elsewhere.

8.   CONCLUSIONS AND RECOMMENDATIONS

A case history has been described where Class C and off-specification cementitious fly ashes (10% by weight) were used to stabilize road-surface gravel (RSG) during construction of a flexible pavement. California bearing ratio (CBR) and resilient modulus (M_r) tests were conducted on the RSG alone and fly-ash stabilized RSG (S-RSG) mixed in the field and laboratory to evaluate how addition of fly ash improved the strength and stiffness. *In situ* testing was also conducted on the subgrade and S-RSG with a soil stiffness gauge (SSG) and dynamic cone penetrometer (DCP). Falling weight deflectometer (FWD) test were conducted after paving on two different occasions. A pan lysimeter was installed beneath the pavement to monitor the rate of drainage and trace element concentrations in the leachate. Two column leaching tests were also conducted on samples of S-RSG collected during construction.

After 7 d of curing, the S-RSG prepared in the laboratory using materials sampled during construction had CBR mostly ranging between 48 and 90, M_r between 96 and 195 MPa, and unconfined compressive strengths between 197 and 812 kPa, whereas the RSG alone had CBR of 24 and M_r of 51 MPa. Field-mix S-RSG had significantly higher CBR and M_r than RSG that was not stabilized with fly ash. This finding suggests that fly ash stabilization of RSG should be beneficial in terms of increasing pavement capacity and service life. The CBRs of S-RSG mixed in the field were mostly 50 to 80 and lower than that for S-RSG mixed in the laboratory (154); however, the opposite was observed for M_r, and for q_u. This is in contrast with previous experience and being explored further.

Moduli obtained from the FWD inversion are compared with those obtained from the resilient modulus tests on field-mix specimens and the moduli computed from the stiffness measured with the SSG. Moduli obtained from the resilient modulus test on

field-mix samples are markedly lower than those obtained from November 2005 FWD but comparable to those from May 2006 FWD. SSG gives 50% higher moduli compared to the modulus obtained from the resilient test . November 2005 FWD data appear anomalously high compared to other data here and elsewhere. Longer-term monitoring is needed to confirm that the modulus of S-RSG will persist after multiple winter seasons.

Chemical analysis of the draining leachate showed that the concentrations of many trace elements were reasonably steady toward the end of the monitoring period. Longer-term monitoring is needed to fully understand the potential for S-RSG to leach trace elements during the service life of a pavement. However, during the monitoring period, all of the concentrations (with the exception of Mn) were below USEPA maximum contaminant levels (MCLs) and Minnesota health risk levels (HRLs) established by the Minnesota Dept. of Public Health. The trace element concentrations in the CLT effluent typically are higher than concentrations in the drainage collected in the field in the lysimeters. The poor agreement suggests that the CLT test method that was used may not be appropriate for evaluating leaching of trace elements from S-RSG, unless a conservative estimate of the trace element concentrations is acceptable. Despite the higher concentrations obtained from the CLT, most of the elements have concentrations below USEPA MCLs and Minnesota HRLs. The exceptions are for B, Be, Cr, Ba,As, and Se. Additional study is also needed to define laboratory leach testing protocols that can more accurately simulate leaching of trace elements from S-RSG.

9. REFERENCES

Benson, C.H. and Bosscher, P.J., 1999. Time-domain reflectometry in geotechnics: a review. In: W. Marr and C. Fairhurst (Editors), Nondestructive and Automated Testing for Soil and Rock Properties, ASTM STP 1350. ASTM International, West Conshohocken, PA, pp. 113-136.

Bin-Shafique, S., Benson, C.H., Edil, T.B. and Hwang, K., 2006. Leachate concentrations from water leach and column leach tests on fly-ash stabilized soils. Environmental Engineering 23(1), pp. 51-65.

Bin-Shafique, S., Edil, T.B., Benson, C.H. and Senol, A., 2004. Incorporating a fly-ash stabilised layer into pavement design. Geotechnical Engineering, Institution of Civil Engineers, United Kingdom, 157(GE4), pp. 239-249.

Edil, T.B., Acosta, H.A. and Benson, C.H., 2006. Stabilizing soft fine-grained soils with fly ash. Journal of Materials in Civil Engineering, 18(2), pp. 283-294.

Edil, T.B. et al., 2002. Field evaluation of construction alternatives for roadways over soft subgrade. Transportation Research Record, No. 1786: National Research Council, Washington DC, pp. 36-48.

Hunt, Roy E. 1986. "Geotechnical Engineering Techniques and Practices." McGraw Hill Book Company.

Li, L., Benson, C. H., Edil, T.B. and Hatipoglu, B. 2006. "Fly Ash Stabilization of Recycled Asphalt Pavement Material in Waseca, Minnesota." Geo Engineering Report N0. 06-18, Department of Civil and Environmental Engineering, University of Wisconsin-Madison.

Powell, W. D., Potter, J. F., Mayhew, H. C., and Nunn, M. E. 1984. "The Structural Design of Bituminous Roads." TRRL Laboratory Report 1132, Transportation and Road Research Laboratory, Crowthorne, Berkshire, 1984, 62 pp.

Rosa, M. "Effect of Freeze-Thaw Cycling on Soils Stabilized with Fly Ash." M.S. Thesis, Department of Civil and Environmental Engineering, University of Wisconsin-Madison, 2006.

Tanyu, B., Kim, W., Edil, T., and Benson, C., 2003. Comparison of laboratory resilient modulus with back-calculated elastic modulus from large-scale model experiments and FWD tests on granular materials. Resilient Modular Testing for Pavement Components, American Society for Testing and Materials, West Conshohocken, PA. STP 1437, pp. 191-208.

Trzebiatowski, B., Edil, T.B. and Benson, C.H., 2004. Case study of subgrade stabilization using fly ash: State Highway 32, Port Washington, Wisconsin. In: A. Aydilek and J. Wartman (Editors), Beneficial Reuse of Waste Materials in

Geotechnical and Transportation Applications, GSP No. 127. ASCE, Reston, VA, pp. 123-136.

Turner, J.P., 1997. Evaluation of western coal fly ashes for stabilization of low-volume roads, Testing Soil Mixed with Waste or Recycled Materials. American Society for Testing and Materials, West Conshohocken, PA. STP 1275, pp. 157-171.

Table 1. Physical properties of subgrade soils.

Station	γ_d (kN/m^3)	w_n (%)	SSG Stiffness (MN/m)	DCP Index (DPI) (mm/blow)	CBR (%)	Elastic Modulus (MPa)*
10+00	19	12	12	14	15	100
20+00	17	3	8	31	6	57
27+30	18	15	14	19	11	81
40+00	18	6	8	30	7	61
50+00	21	8	13	39	5	48
60+00	19	12	17	19	11	81
70+00	22	7	12	7	33	165
80+00	20	8	9	9	25	138
90+00	19	5	8	16	13	91
104+00	19	5	9	20	10	78

Notes: SSG = Soil Stiffness Gauge, DCP = Dynamic Cone Penetrometer (DPI is the weighted average DPI over a depth of 150 mm), CBR = California Bearing Ratio (estimated from weighted DPI), w_n = in situ water content and γ_d = in situ dry unit weight (measured by nuclear gauge).
* Estimated from CBR

Table 2. Index properties and classification of subgrade soils.

Group	Stations	LL	PI	% Fines	GI	USCS Group Symbol	USCS Group Name	AASHTO
A	20+00 40+00	NP	NP	6.9	0	SP-SM	Poorly graded sand with silt	A-3
B	27+30 60+00	44	28	61.8	14	CL	Sandy lean clay	A-5
C	50+00 70+00 80+00 104+00	18	NP	21.1	0	SM	Silty sand	A-2-4
D	10+00	21	4	53.8	0	CL-ML	Sandy silty clay	A-4
E	90+00	NP	NP	16.5	0	SM	Silty sand	A-2-4

Note: LL = liquid limit. PI = plasticity index. GI = AASHTO group index. USCS = Unified Soil Classification System. AASHTO = American Association of State Highway and Transportation Officials.

Table 3. Grain size fractions, in situ water content, and compaction characteristics of RSG.

Station	% Gravel	% Sand	% Fines	D_{10} (mm)	C_u	C_c
10+00	27.8	58.6	13.6	0.03	38	1.6
20+00	18.4	69.5	12.0	0.05	17	1.6
27+30	28.1	60.8	11.2	0.06	30	0.8
40+00	22.4	64.9	12.8	0.06	19	1.1
50+00	25.9	62.1	12.0	0.06	21	1.1
60+00	20.8	64.4	14.8	0.04	21	1.8
70+00	19.5	68.4	12.1	0.05	16	1.7
80+30	32.8	55.4	11.8	0.10	5	1.1
90+00	20.1	57.5	22.4	0.03	13	1.7
104+00	16.8	69.7	13.5	0.03	25	1.6
Composite	24.5	64.3	11.2	0.06	20	0.9

Notes: D_{10} = effective grain diameter, C_u = uniformity coefficient, C_c = coefficient of curvature.

Table 4. Types of fly ashes used in each station.

Station	Fly Ash Type
10+00	Riverside 7, Riverside 8
20+00	Riverside 7, Riverside 8
27+30	Riverside 8
40+00	Riverside 7
50+00	Riverside 7, Riverside 8
60+00	Riverside 8
70+00	Riverside 8
80+30	Riverside 7, Riverside 8
90+00	-
104+00	-

Table 5. Chemical composition and physical properties of Riverside 7 and 8 fly ashes, typical Class C and F fly ashes, and specifications for Class C fly ash

Parameter	Percent of Composition				Specifications	
	Riverside 7[+]	Riverside 8[+]	Typical* Class C	Typical* Class F	ASTM C 618 Class C	AASHTO M 295 Class C
SiO_2 (silicon dioxide), %	32	19	40	55		
Al_2O_3 (aluminum oxide), %	19	14	17	26		
Fe_2O_3 (iron oxide), %	6	6	6	7		
$SiO_2 + Al_2O_3 + Fe_2O_3$, %	57	39	63	88	50 Min	50 Min
CaO (calcium oxide), %	24	22	24	9		
MgO (magnesium oxide), %	6	5.5	2	2		
SO_3 (sulfur trioxide), %	2	5.4	3	1	5 Max	5 Max
CaO/SiO_2	0.75	1.18				
$CaO/(SiO_2+Al_2O_3)$	0.47	0.68				
Loss on Ignition, %	0.9	16.4	6	6	6 Max	5 Max
Moisture Content, %	0.17	0.32	-	-	3 Max	3 Max
Specific Gravity	2.71	2.65	-	-		
Fineness, amount retained on #325 sieve, %	12.4	15.5	-	-	34 Max	34 Max

[+]Chemical analysis and physical analysis provided by Lafarge North America
*from Bin-Shafique et al. (2004)

Table 6. CBR, M_r, and q_u of RSG and S-RSG.

Station	CBR (%)			M_r (MPa)			q_u (kPa)	
	RSG (Lab)	Field-Mix S-RSG	Lab-Mix S-RSG	RSG	Field-Mix S-RSG	Lab-Mix S-RSG	Field-Mix S-RSG	Lab-Mix S-RSG
10+00	-	52	-	-	195	-	288	-
20+00	-	48	-	-	119	-	422	-
27+30	-	78	-	-	175	-	215	-
40+00	-	90	-	-	173	-	812	-
50+00	-	16	-	-	96	-	352	-
60+00	-	50	-	-	150	-	197	-
70+00	-	83	-	-	180	-	490	-
80+30	-	59	-	-	136	-	484	-
90+00	-	-	-	-	-	-	-	-
104+00	-	-	-	-	-	-	-	-
Composite	24	-	154	51[a]	-	80[b]		183

Notes: CBR = California bearing ratio, M_r = resilient modulus, q_u = unconfined compressive strength, hyphen indicates test not conducted, NA = not available because specimen damaged. [a] Tested as granular soil at bulk stress 70 kPa. [b] Reported at deviator stress of 21 kPa.

Table 7. Mr, and qu changes of S-RSG subjected to freeze-thaw cycles.

Freeze-Thaw Cycle	Normalized M_r	Normalized q_u
0	1	1
1	0.94	1.2
3	0.90	2.3
5	0.83	0.97

Notes: M_r = resilient modulus reported at deviator stress of 21 kPa (normalized by M_r of specimen not subjected to freeze-thaw). q_u = unconfined compressive strength (normalized by M_r of specimen not subjected to freeze-thaw). All tests in replicate.
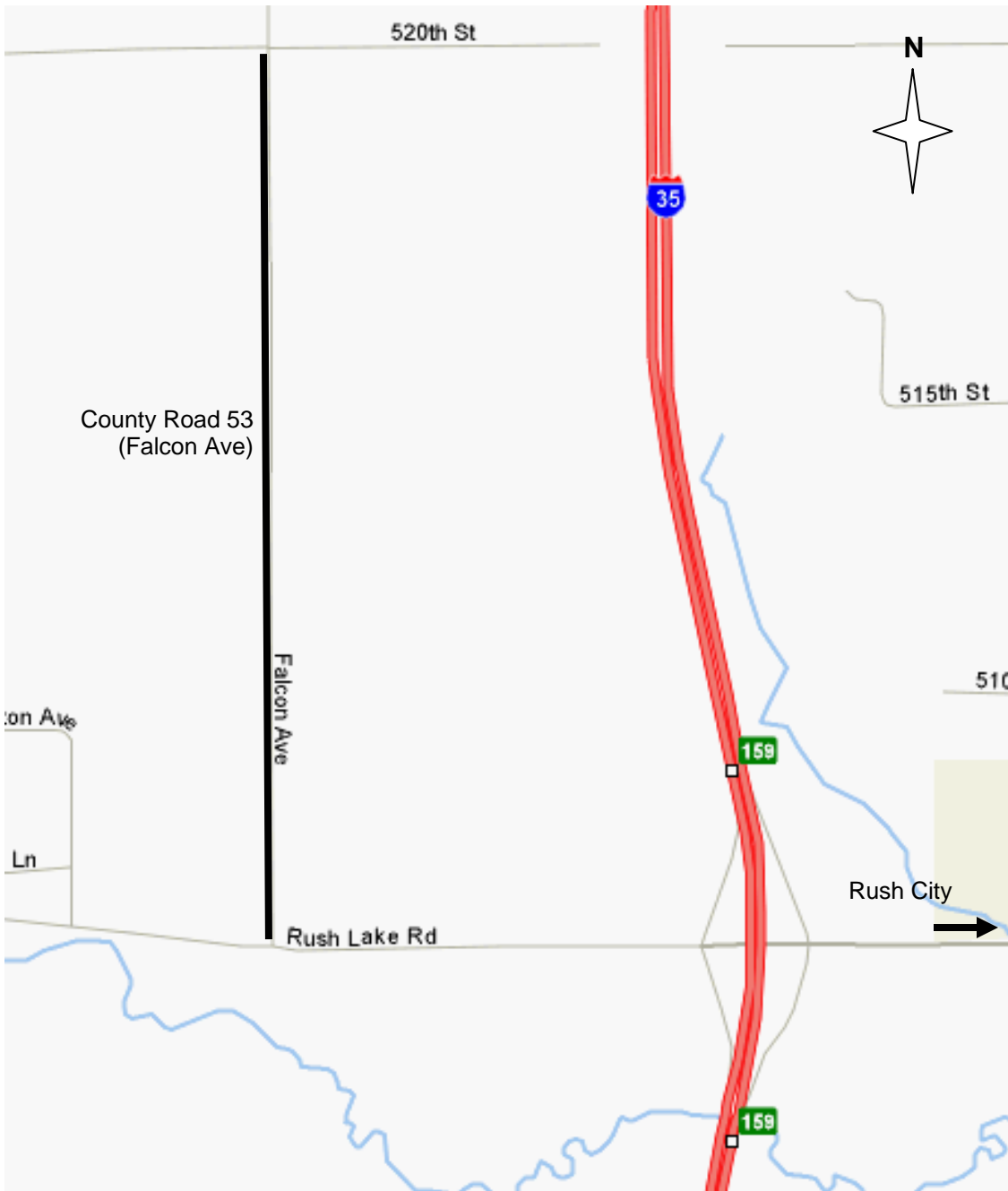
Fig. 1 Location of County Road 53 and study area.

Fig. 2 (a) Spreading of fly ash on gravel road with lay-down equipment and (b) Mixing process of fly ash, road-surface gravel, and water by a reclaimer (compaction is performed right after mixing by tamp-foot compactor seen in the background).
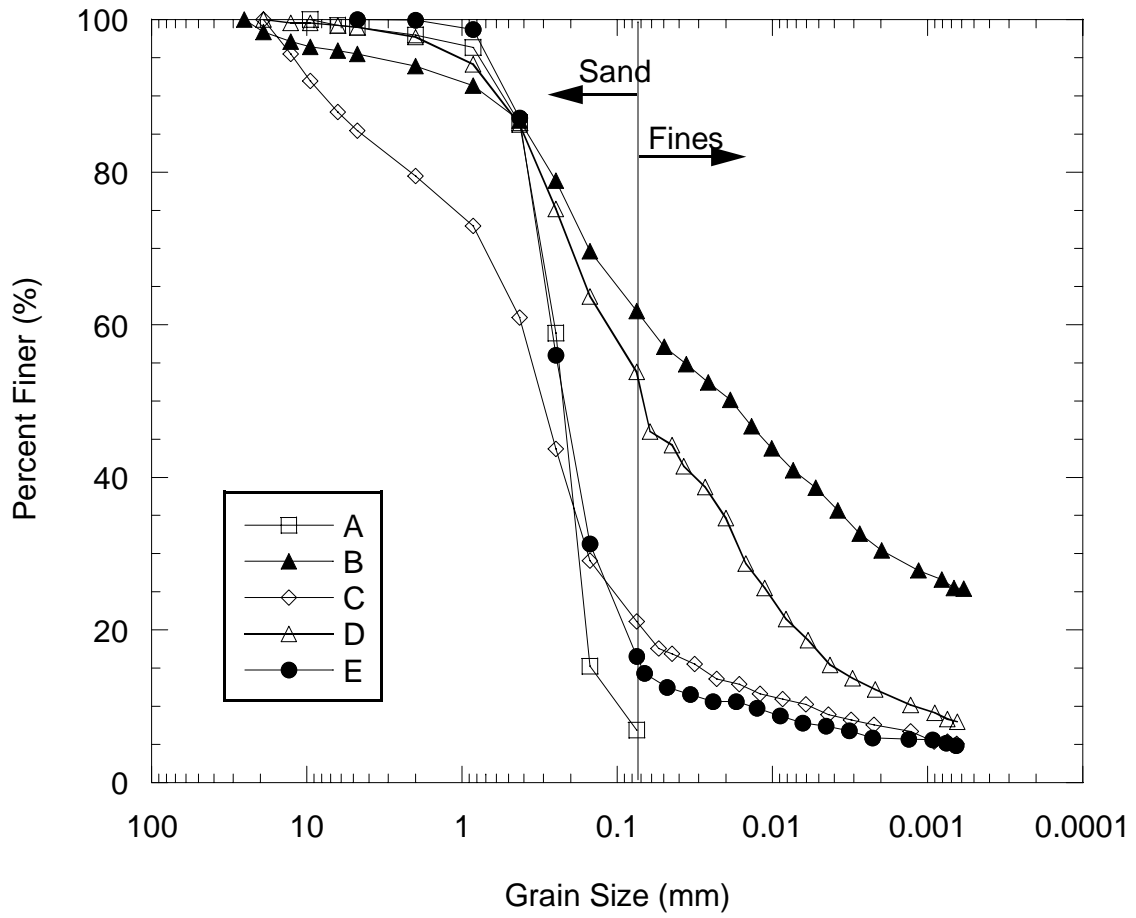
Fig. 3 Grain size distribution curves of grouped subgrade samples.
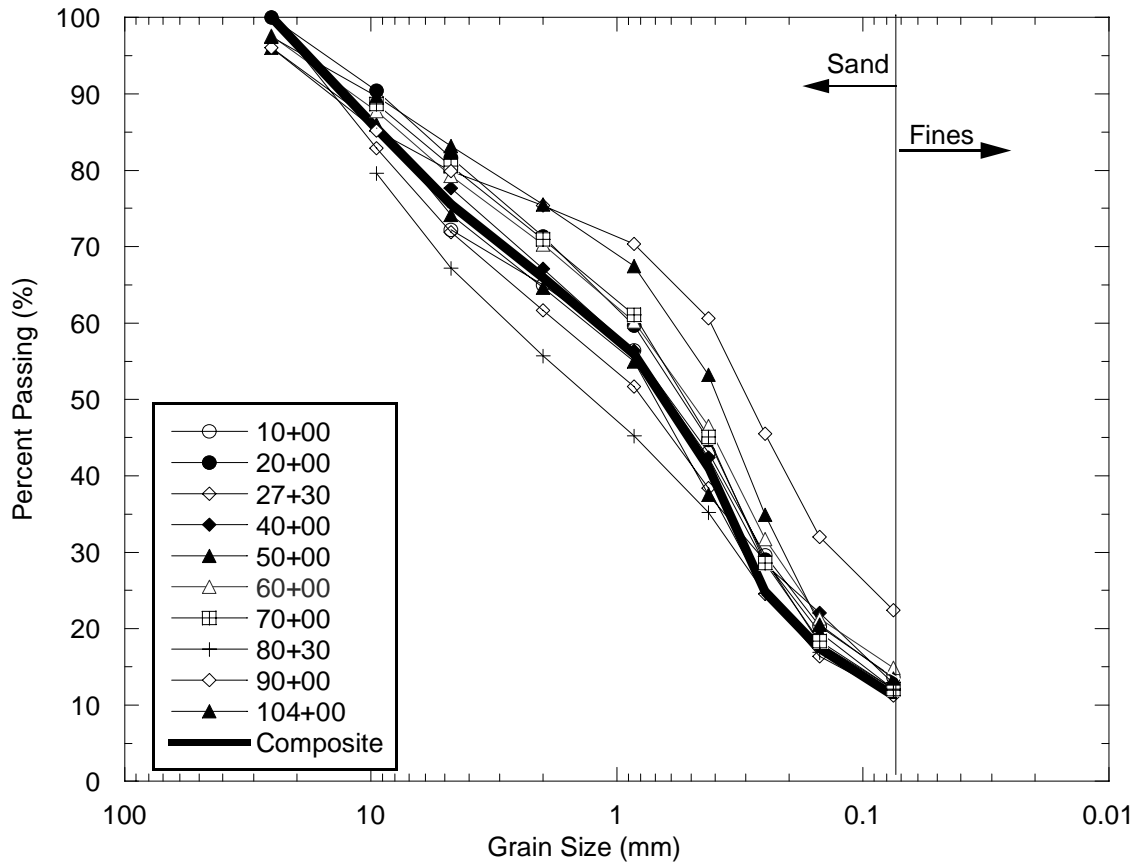
Fig. 4 Grain size distribution curves of RSG at sampling stations and composite of all stations.
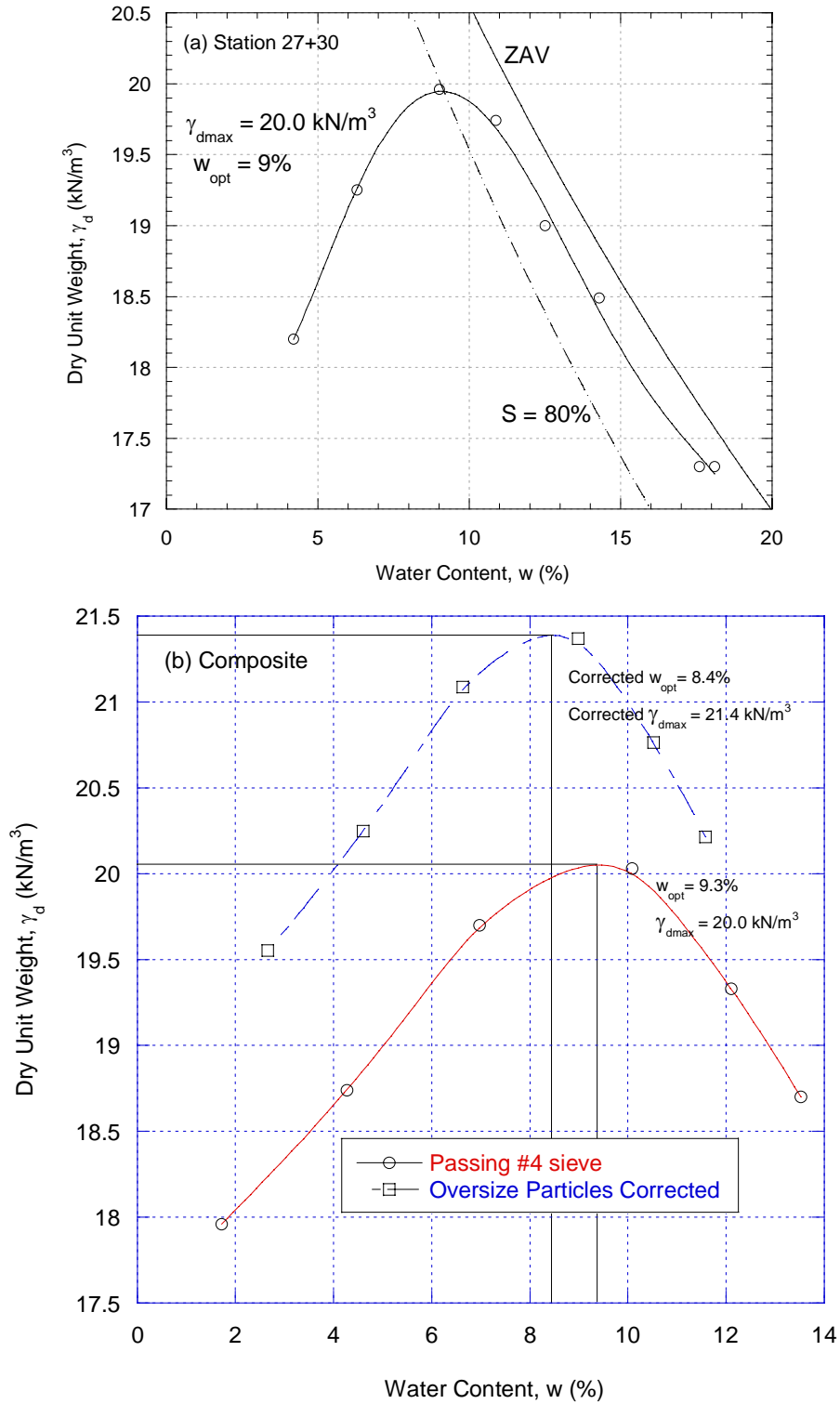
Fig. 5 Compaction curves: (a) for an RSG sample from Station 27+30 and (b) for the composite of RSG samples from of all stations.
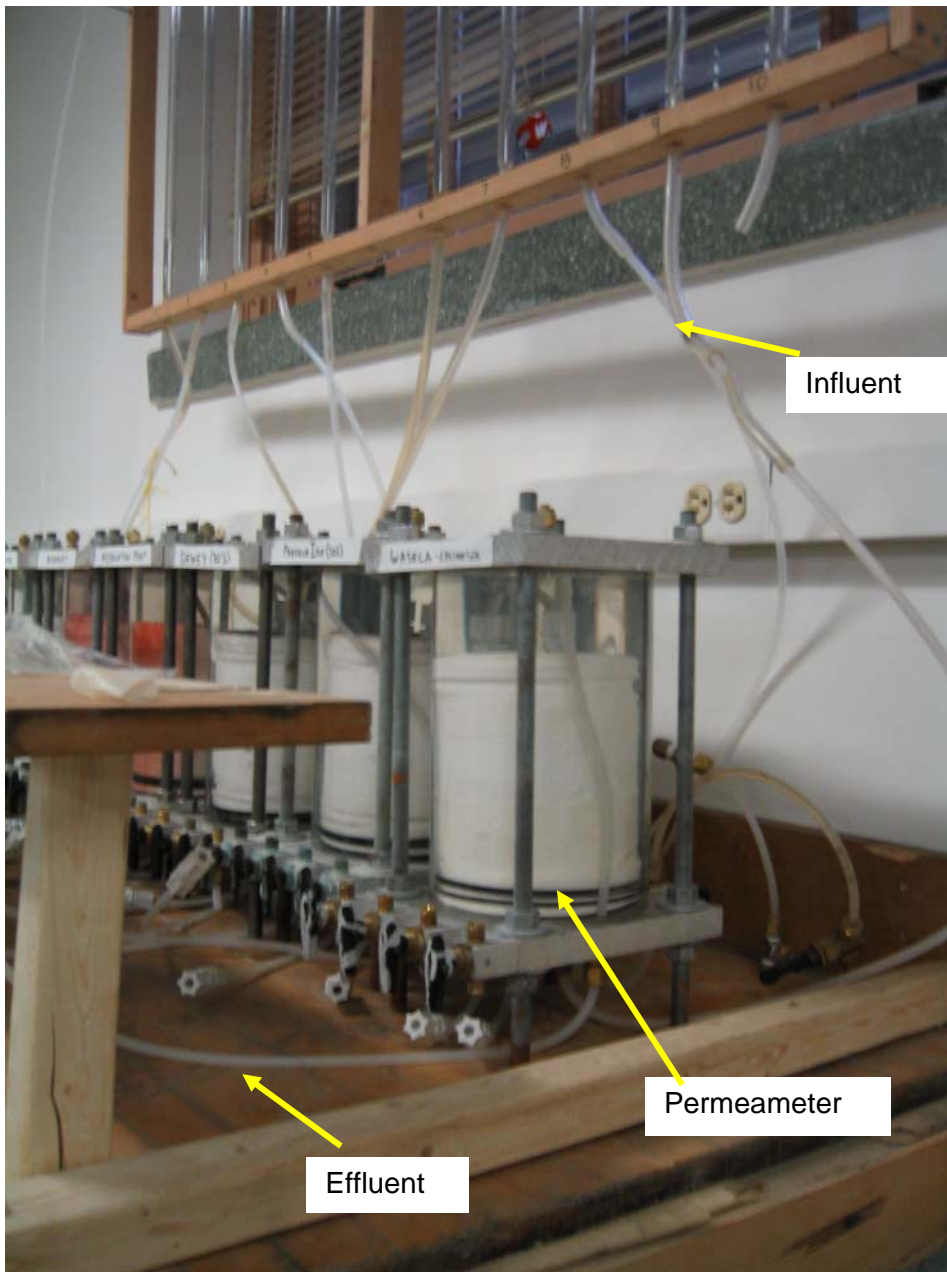
Fig. 6 Column leach test experimental setup

(a) Lysimeter

Collection Tank

(b) Collection Tank

Leachate collection pipes

Pipe from lysimeter
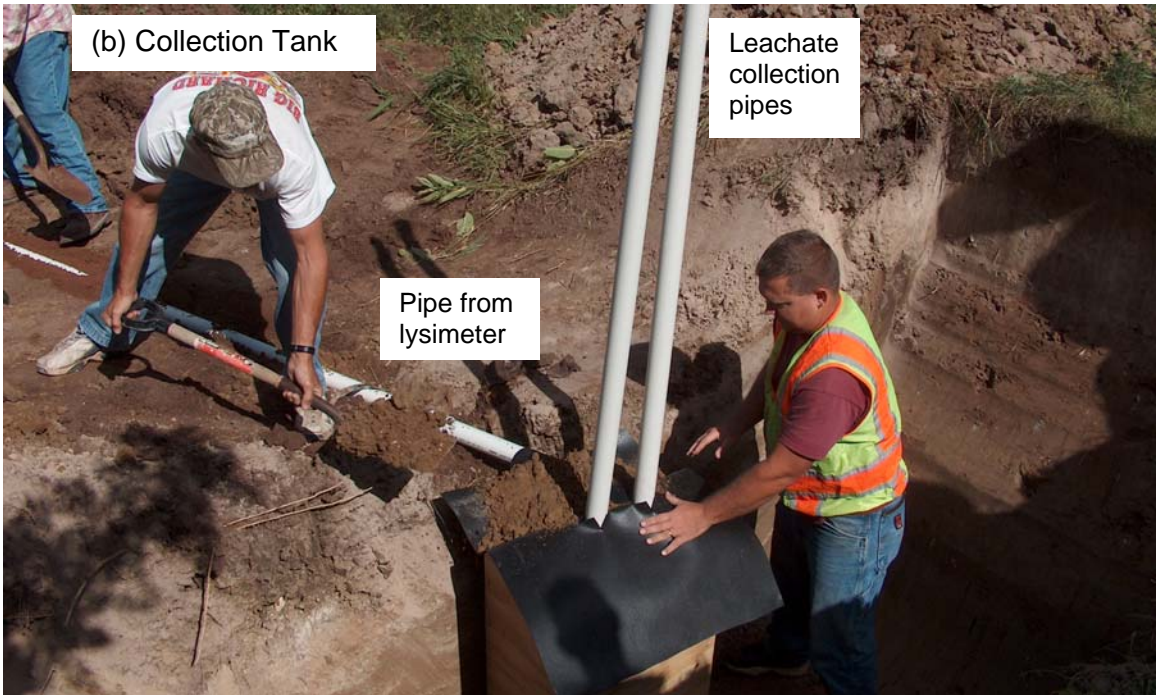
Fig. 7 Construction of Lysimeter (a) and leachate collection tank (b) at St. 27+30.

N

Sensor ID	Depth of sensor from ACP surface (mm)
S1	700.0
S2	445.0
S3	216.0
S4	241.0
S5	420.0
S6	685.0

(a)

Lysimeter

3.05 m

3.90

UW-Sta 3
27+30

Locations of datalogger modem, weather station and solar panel

A (Sensor 1,2)

Sensor 3

3.05 m

B

Sensor 4

C (Sensor 5,6)

2.75

Leachate collection tank

POC line

HMA

Fly-ash mixed gravel

Sensor 3, 4

Gravel

Sensor 5

Sensor 2

Subgrade

Sensor 1

Sensor 6

Volumetric water content & soil temperature gauge

Soil temperature sensor

Lysimeter

Drawing is not in scale

(b)

Solar panel

Rain gauge

Relative humidity and air temperature gauge

CR23X data logger, AM25T multiplexer and COM 200 modem

Lysimeter

STA: UW3 27+3

Battery

Phone line

Fig. 8 (a) Layout (b) Photograph of completed field monitoring instrumentation system.
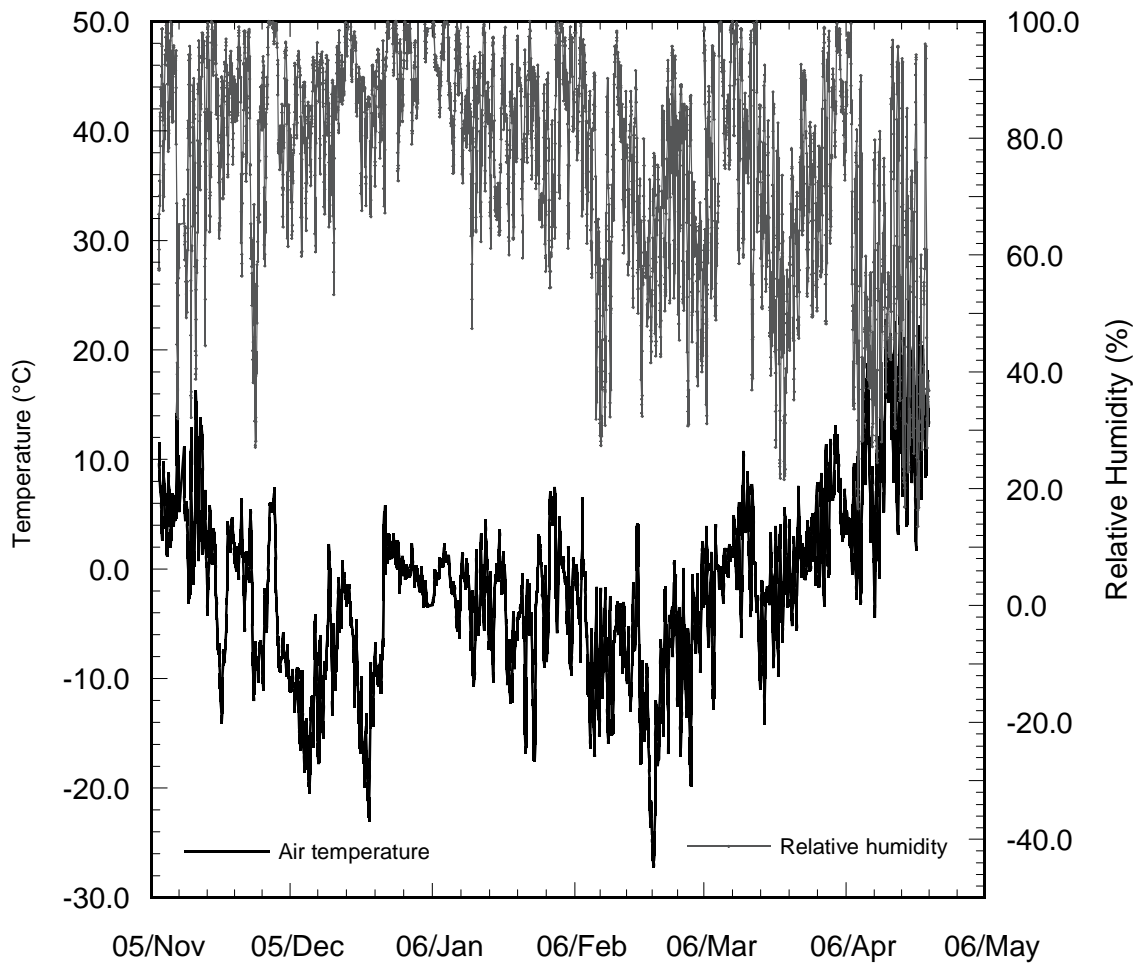
Fig. 9 Air temperature and relative humidity at CR 53.

45
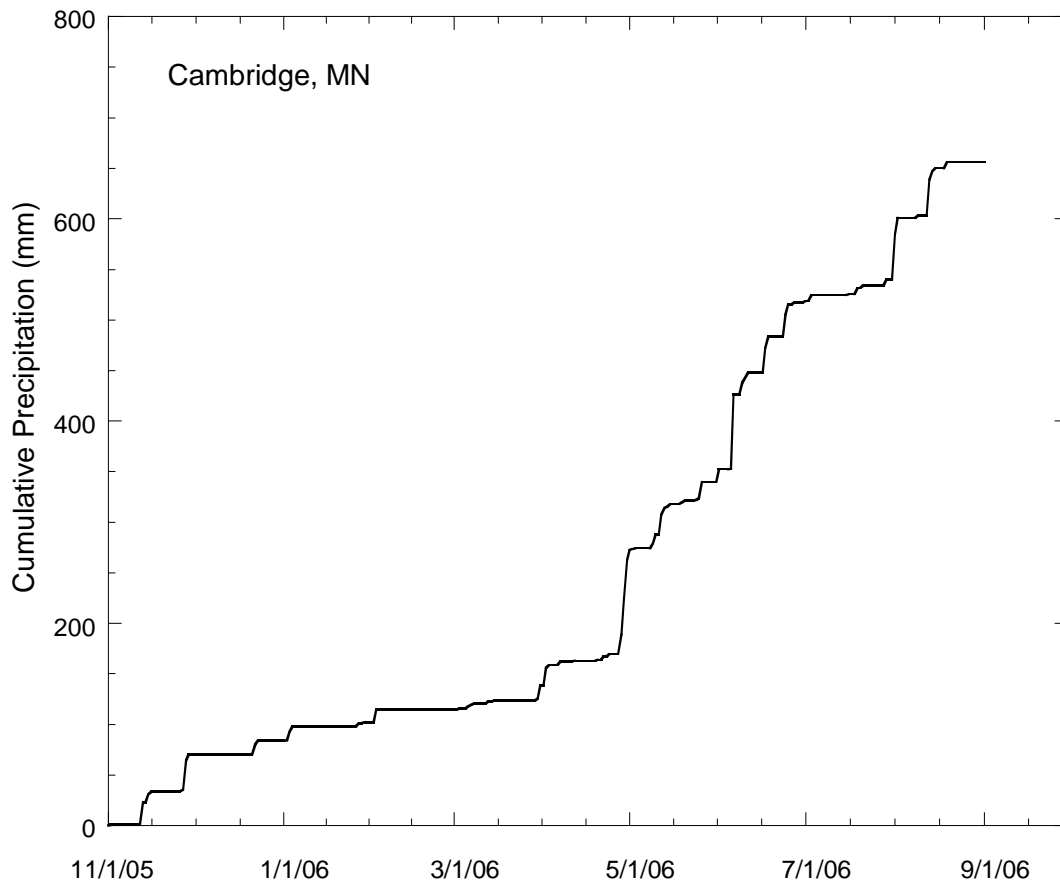
Fig. 10 Cumulative precipitation at Cambridge, MN (nearest NOAA Station to CR 53).
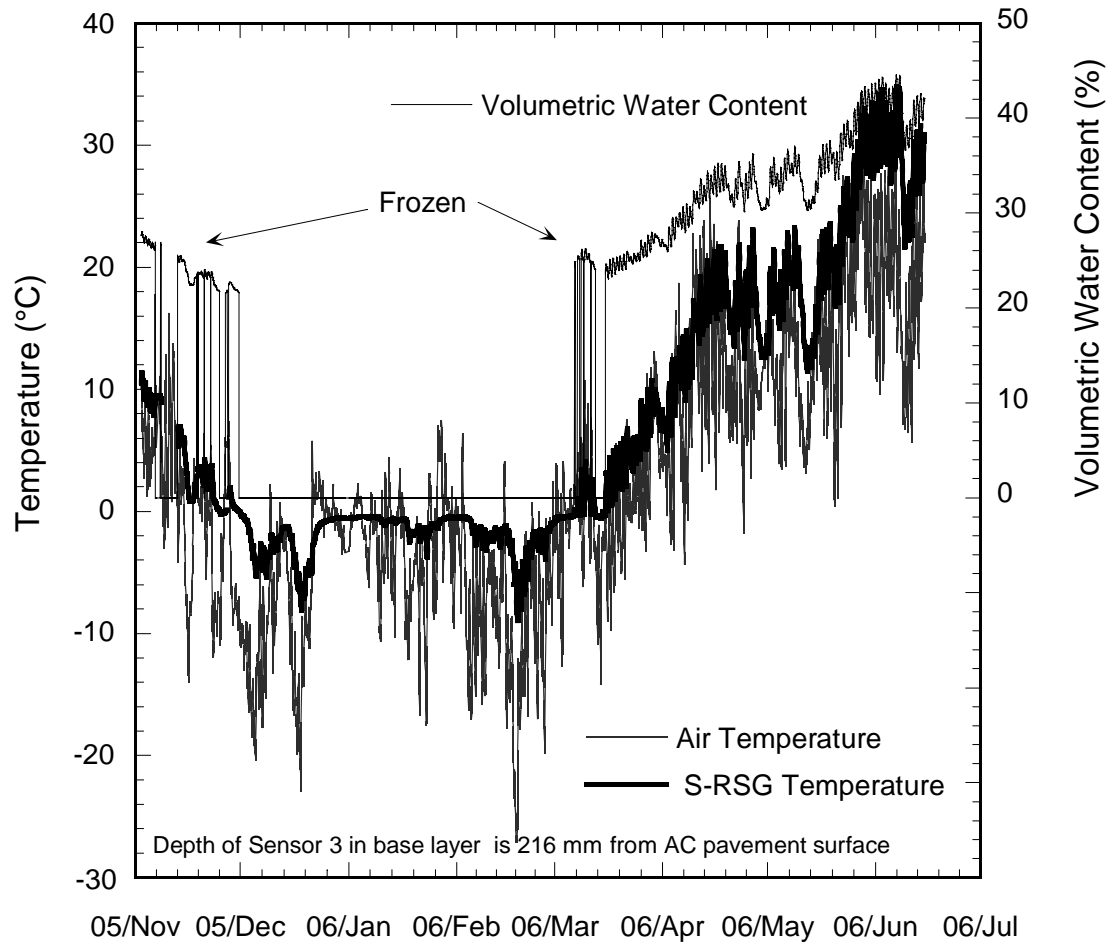
Fig. 11 Soil temperature and volumetric water content measurements in S-RSG layer at 216 mm depth from the AC pavement surface.
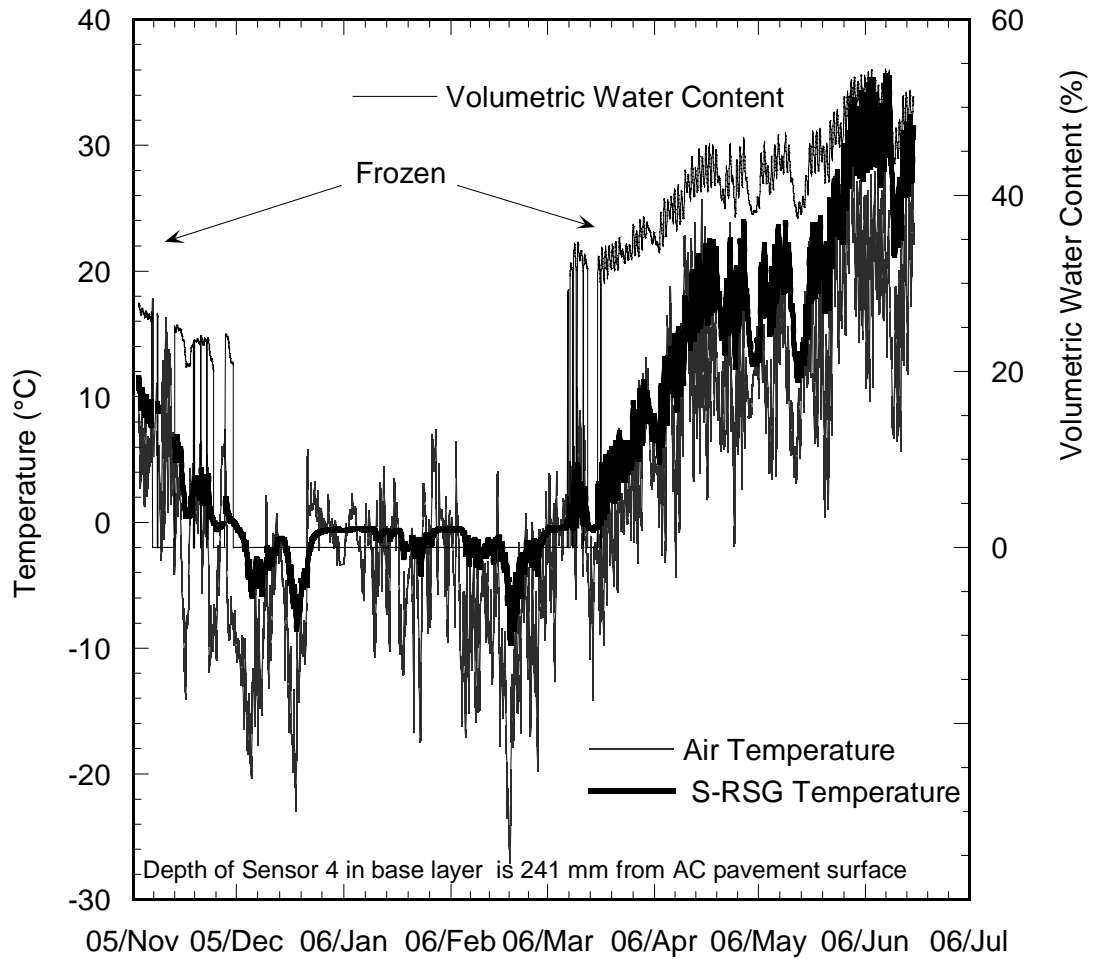
Fig. 12 Soil temperature and volumetric water content measurements in S-RSG layer at 241 mm depth from the AC pavement surface.
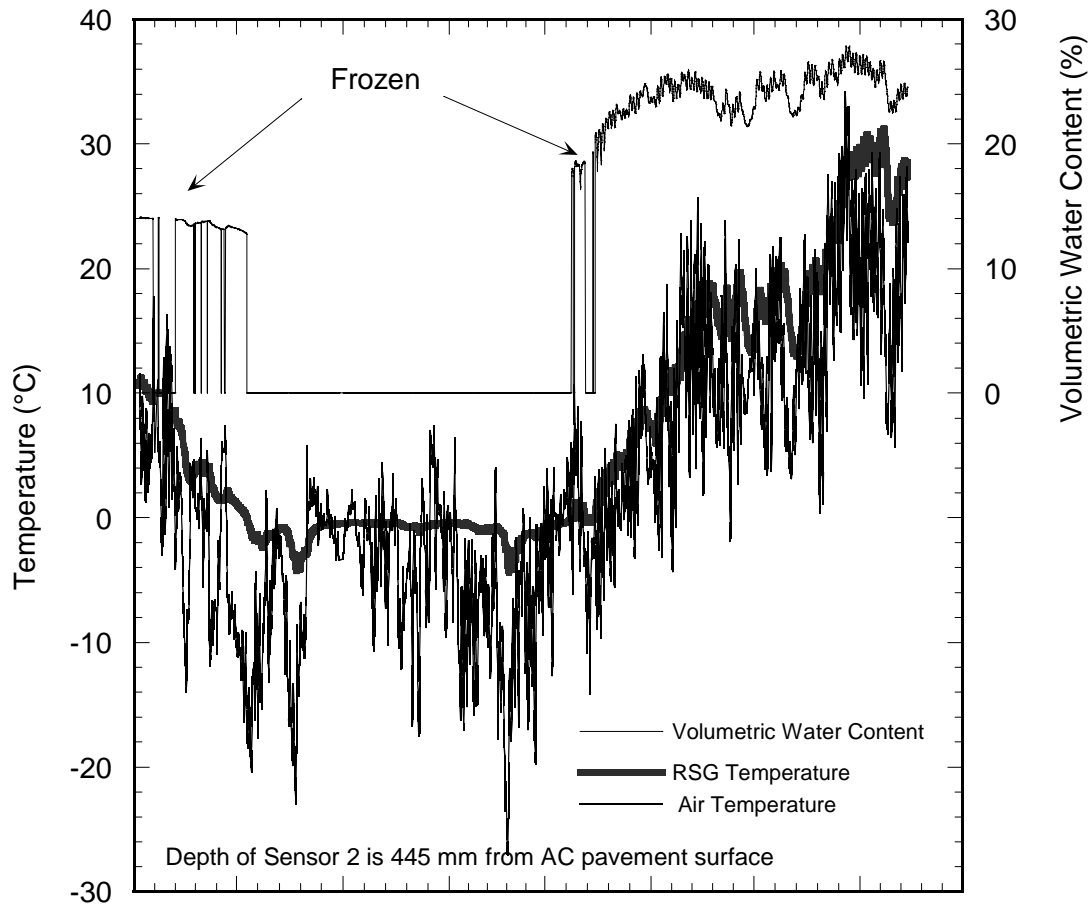
Fig. 13 Soil temperature and volumetric water content measurements in RSG at 445 mm depth from the AC pavement surface.
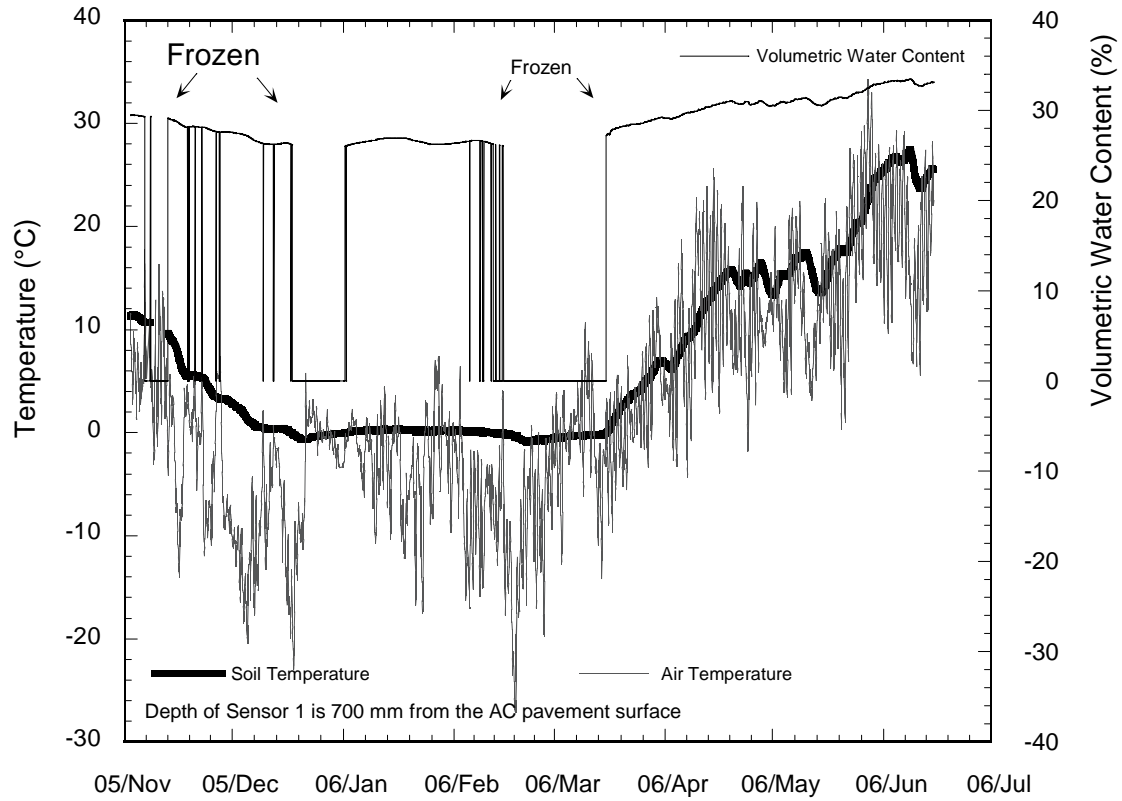
Fig. 14 Soil temperature and volumetric water content measurements in subgrade at 700 mm depth from the AC pavement surface.
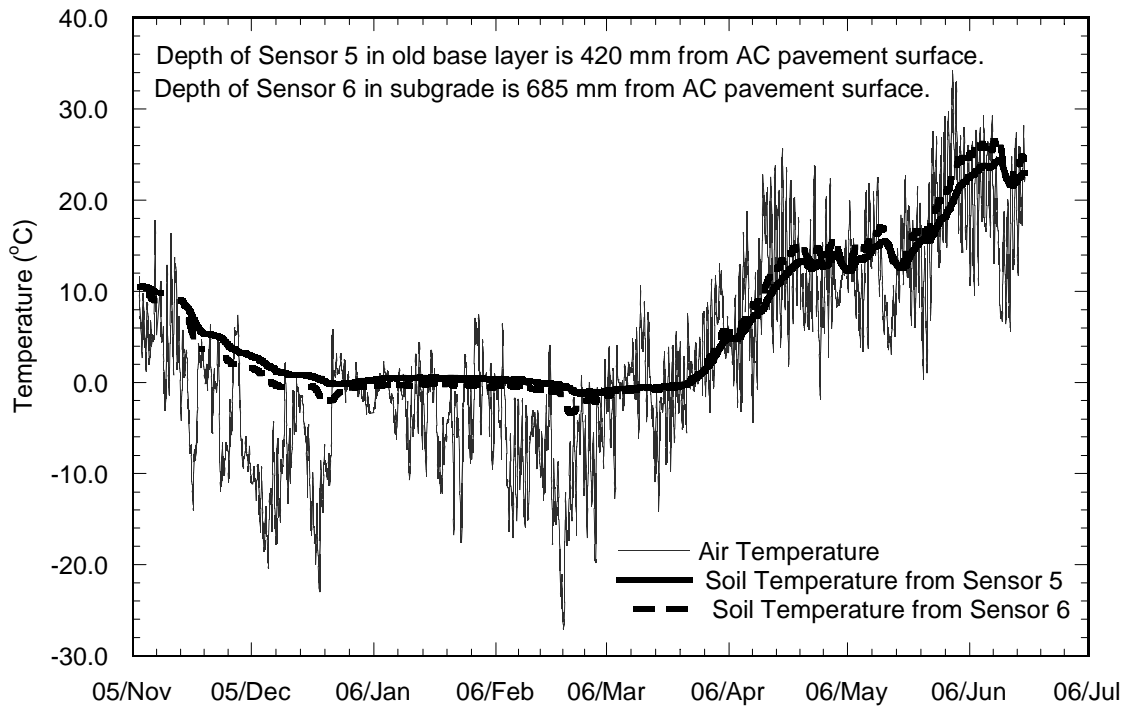
Fig. 15 Soil temperature measurements in RSG at 420 mm depth and in subgrade at 685 mm depth from the AC pavement surface.
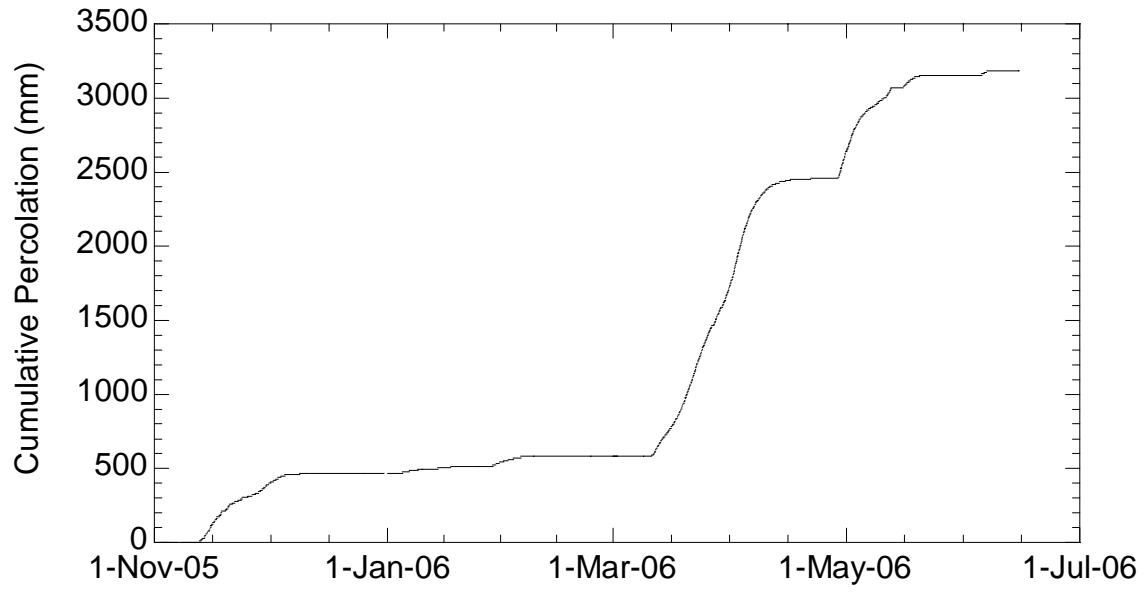
Fig. 16 Cumulative percolation into Lysimeter.
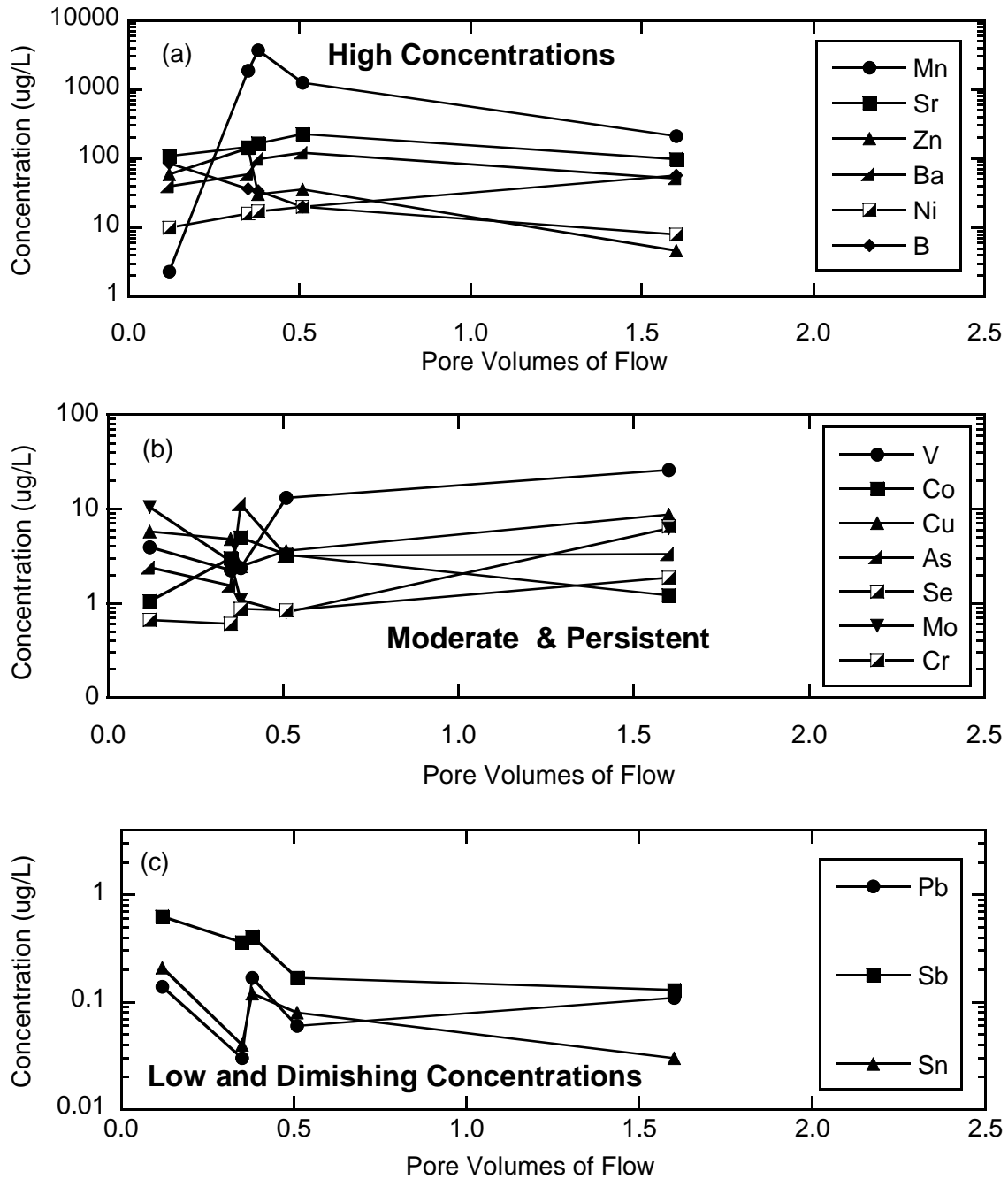
Fig. 17 Concentrations of trace elements in leachate collected in lysimeter: (a) elements with high concentrations, (b) elements with moderate and persistent concentrations and (c) elements with low and diminishing concentrations.
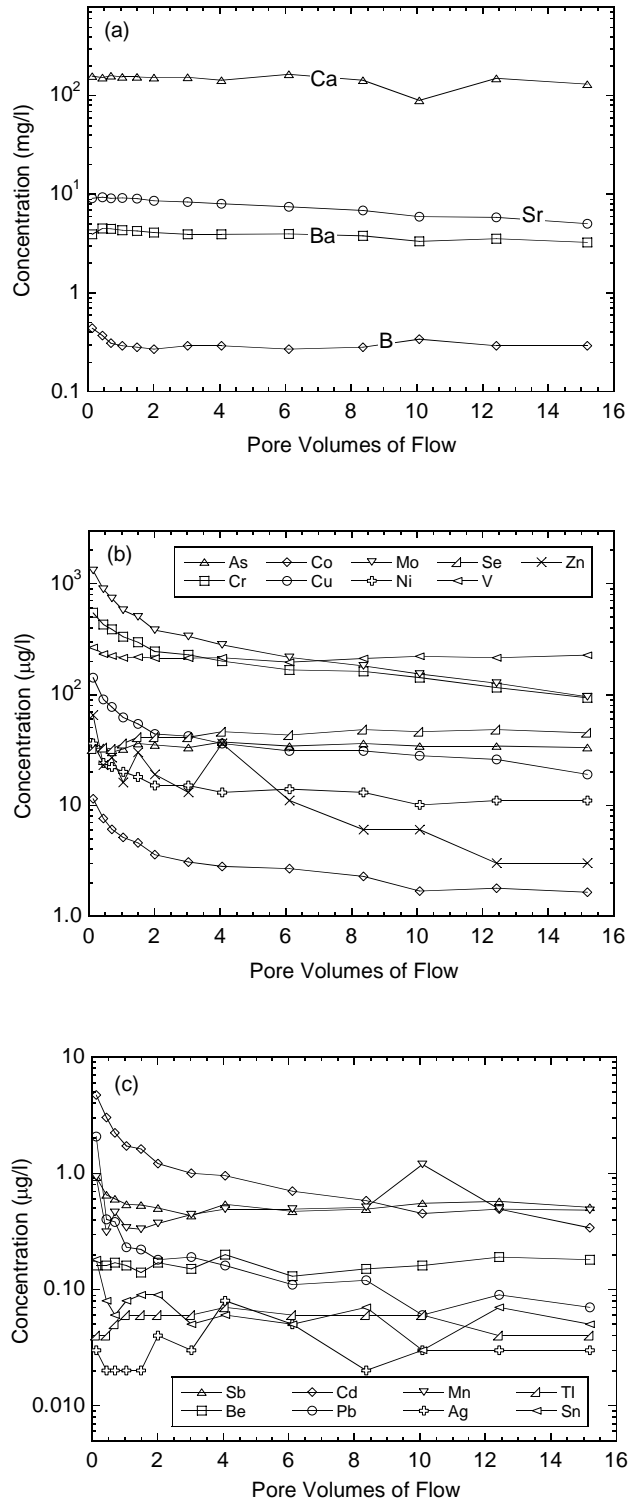
Fig. 18 Concentrations of trace elements in effluent from CLT on CH2 (Chisago Station 2): elements with peak concentrations (a) exceeding 1 mg/L, (b) elements with peak concentrations exceeding 10 μg/L, but less than 1 mg/L, and (c) elements with peak concentrations less than 10 μg/L.
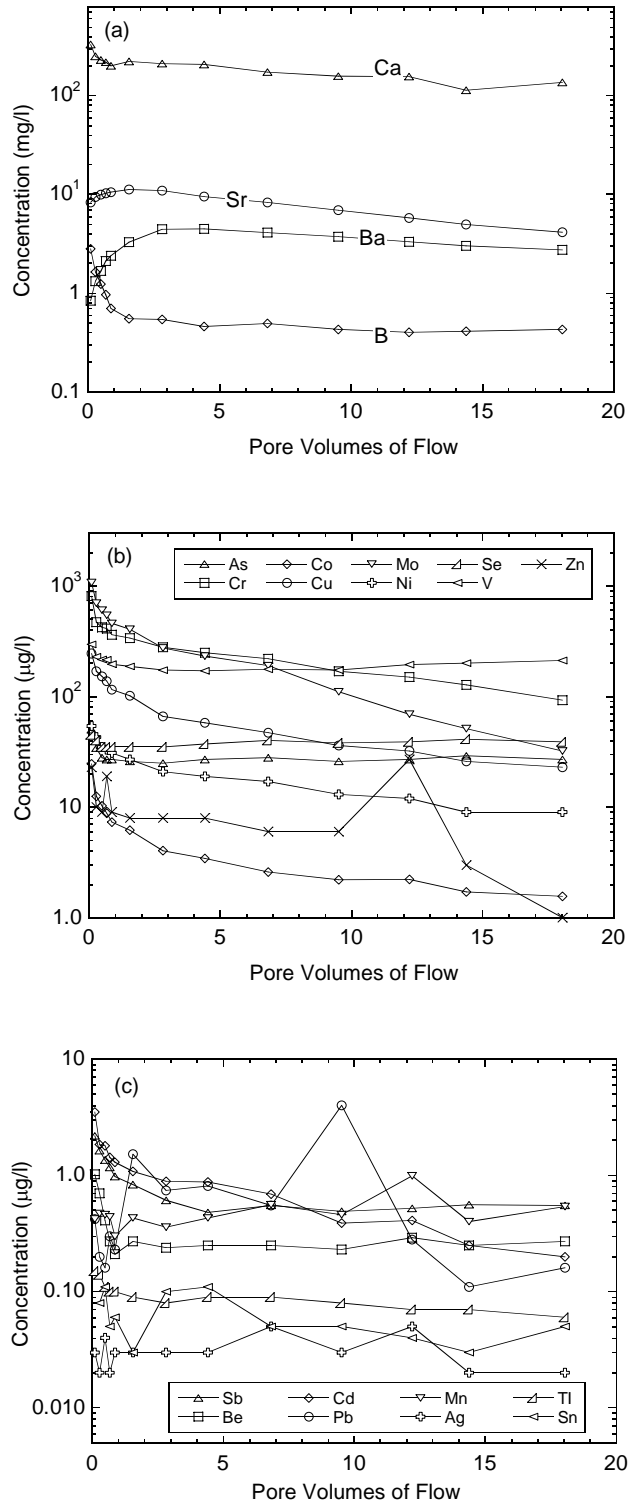
Fig. 19 Concentrations of trace elements in effluent from CLT on CH5 (Chisago Station 5): elements with peak concentrations (a) exceeding 1 mg/L, (b) exceeding 10 μg/L, but less than 1 mg/L, and (c) less than 10 μg/L.
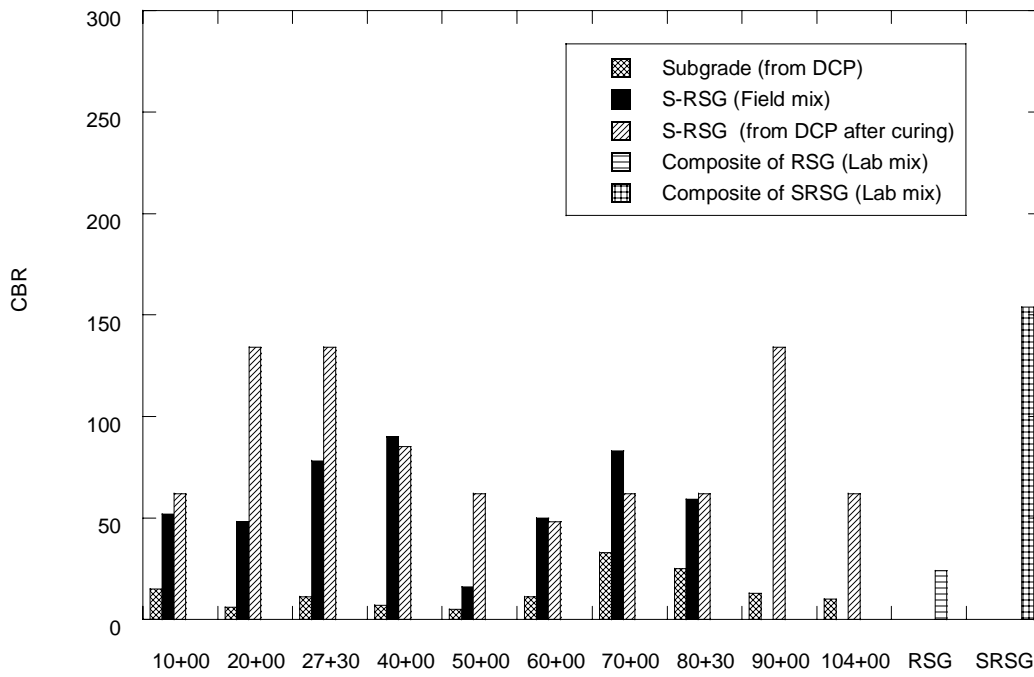
Fig. 20 California Bearing Ratio of S-RSG prepared in the field. Tests performed after 7 days of curing time.
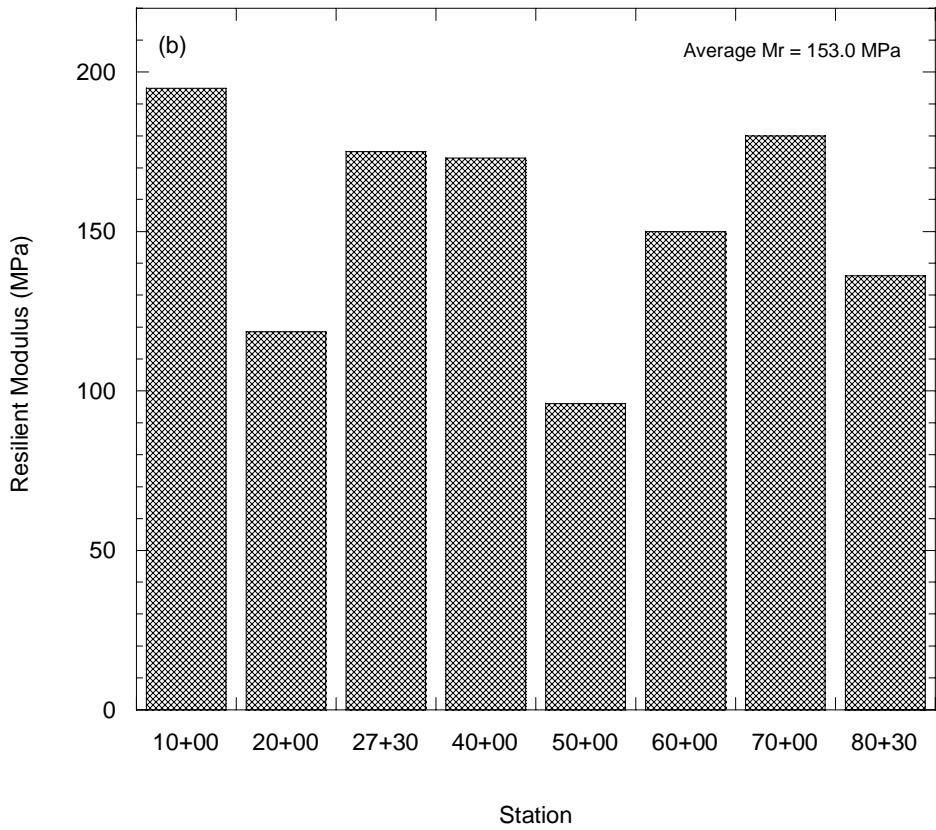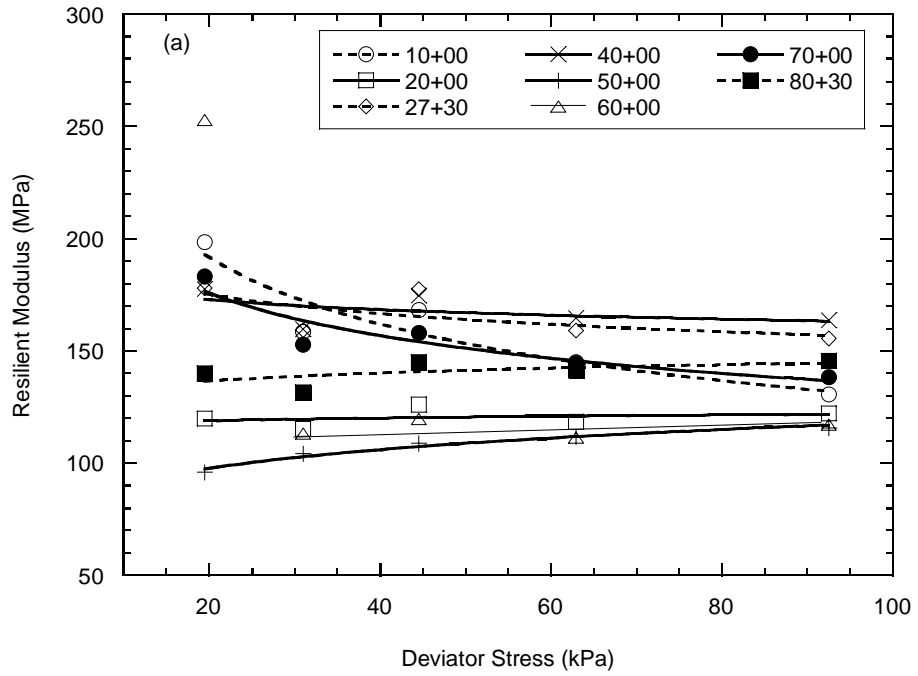
Fig. 21 Resilient modulus of mixture of fly-ash and gravelly soil prepared in the field. Tests performed after 7 days of curing time. (a) Resilient modulus versus deviator stress (b) Resilient modulus values at each station.
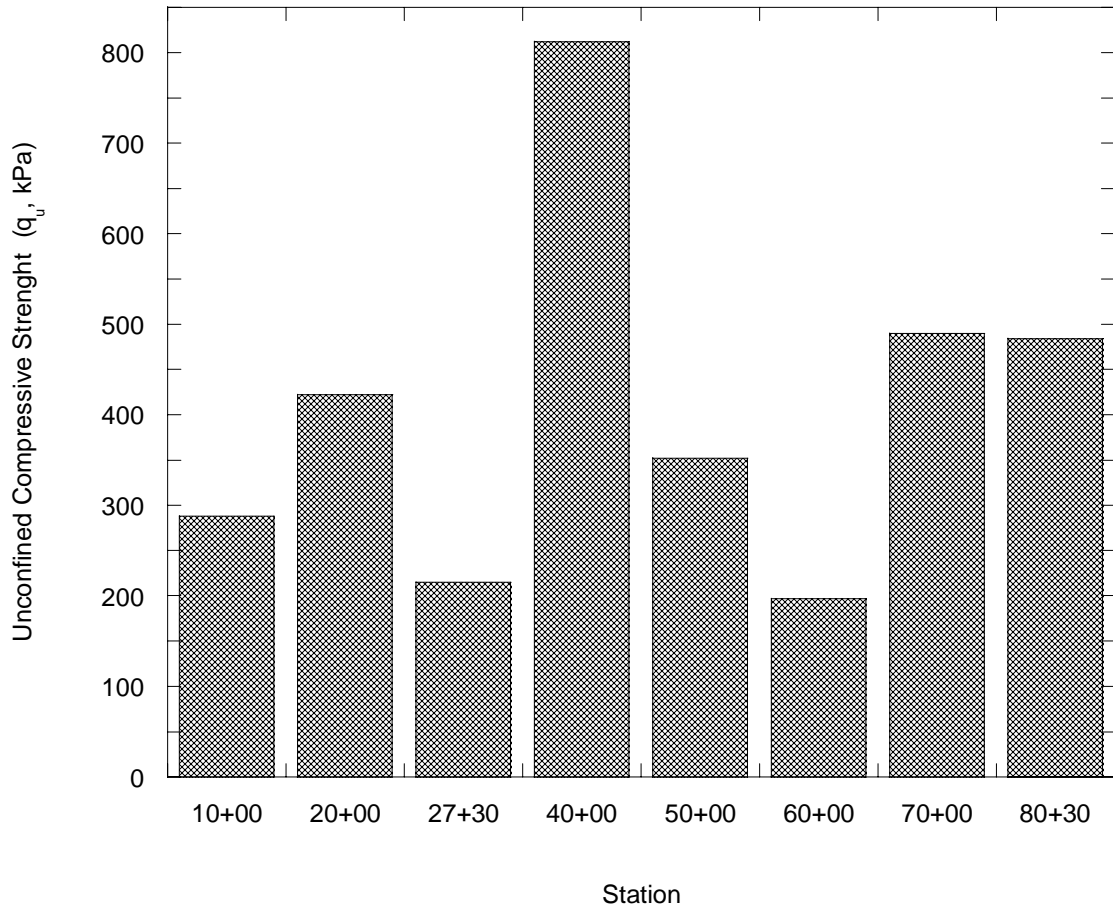
Fig. 22 Unconfined compressive strength (qu) of mixture of fly-ash and gravelly soil prepared in the field. Tests performed after 7 days of curing time.
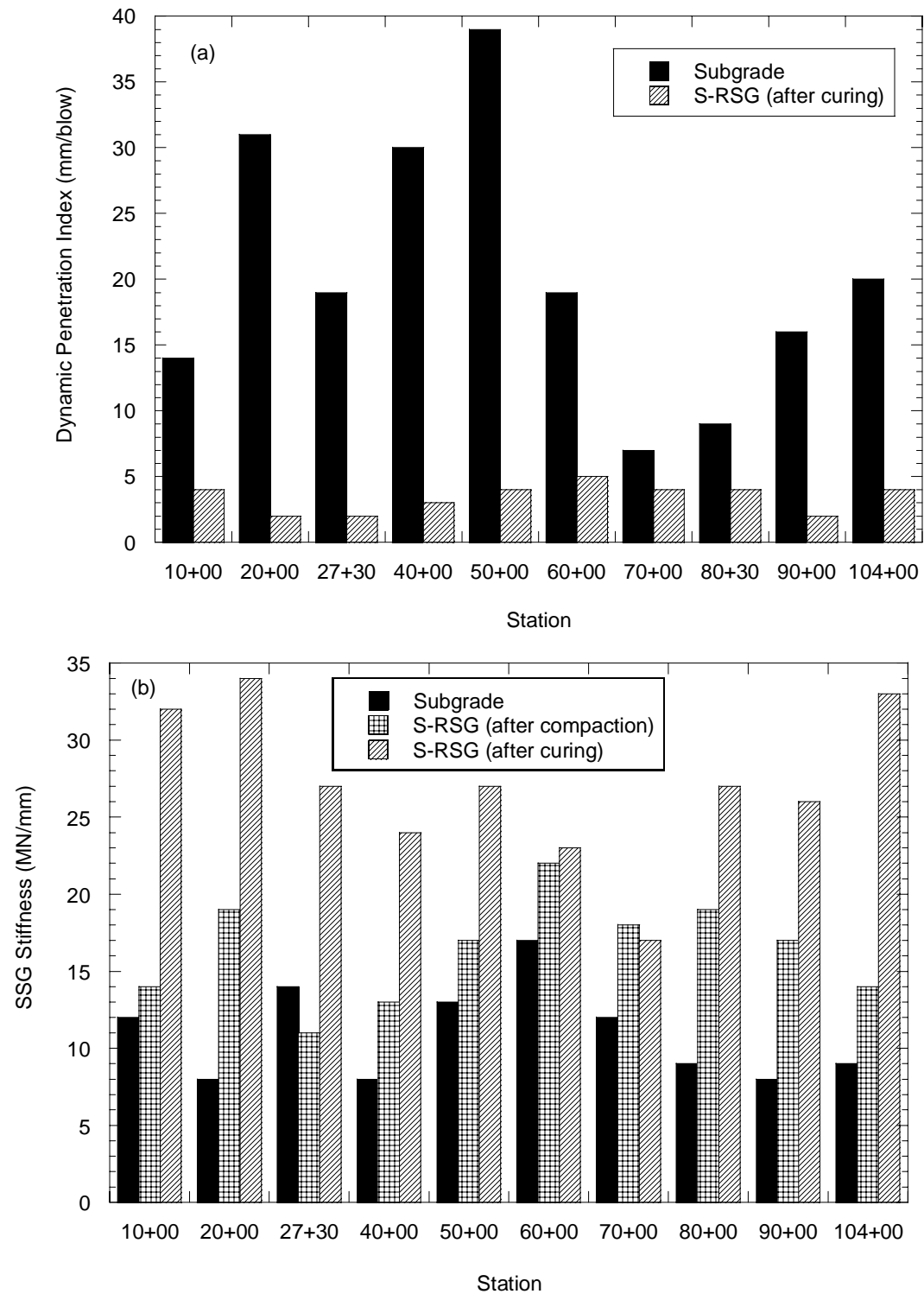
Fig. 23 (a) Dynamic penetration index (DPI) of subgrade and S-RSG soil prepared in the field after 7 days of curing, (b) Soil stiffness gauge stiffness of subgrade, S-RSG after compaction and after 7 of curing
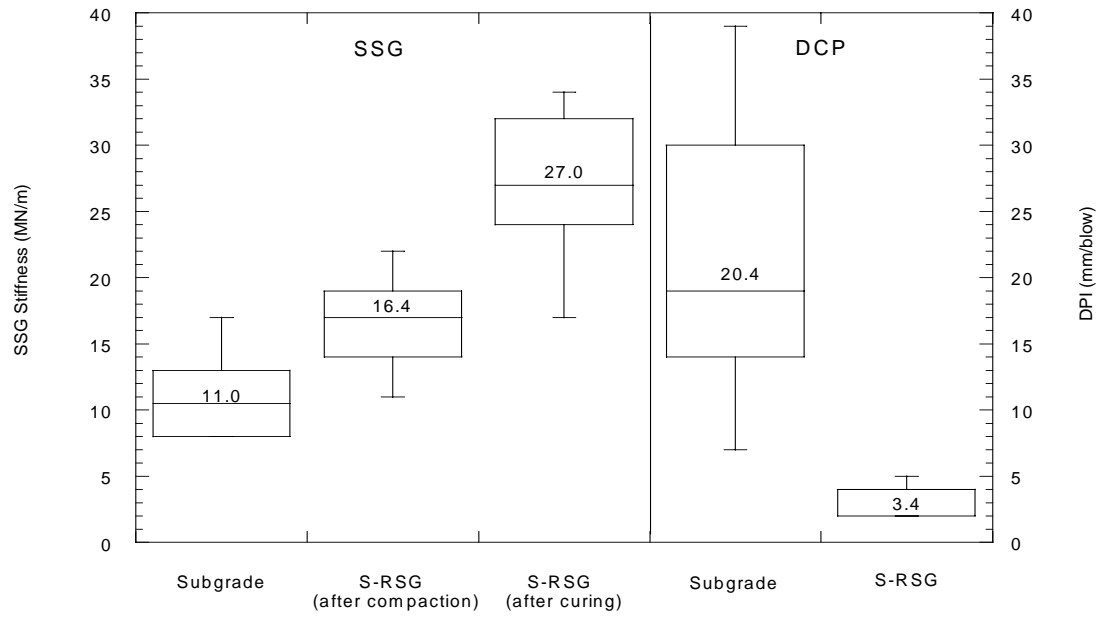
Fig. 24 Statistical evaluation of SSG and DCP test results.
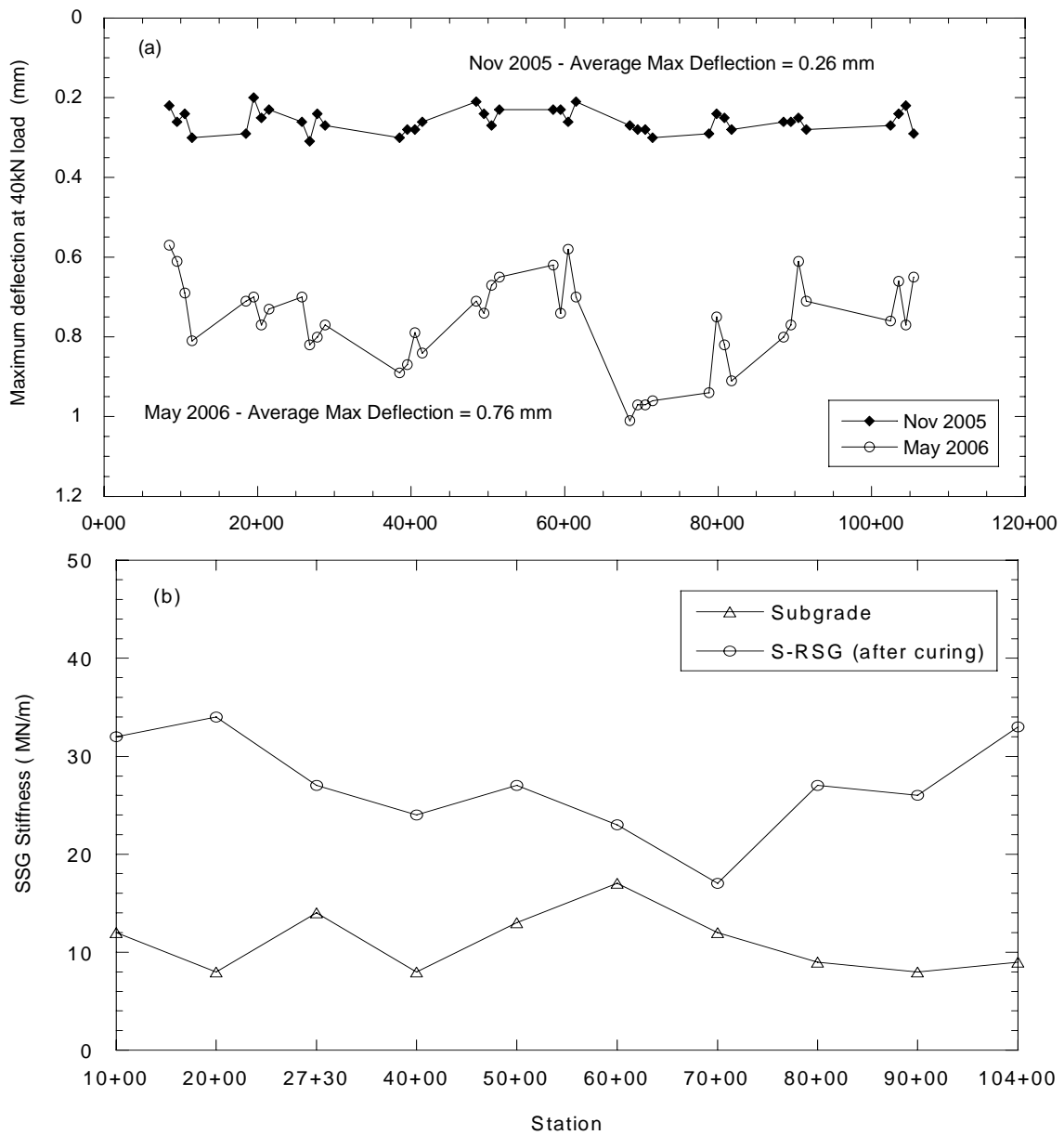
Fig. 25 (a) Maximum deflections -deflections from the center sensor at 40 kN load (b) Soil stiffness gauge stiffness of subgrade, S-RSG after compaction and after 7 days of curing
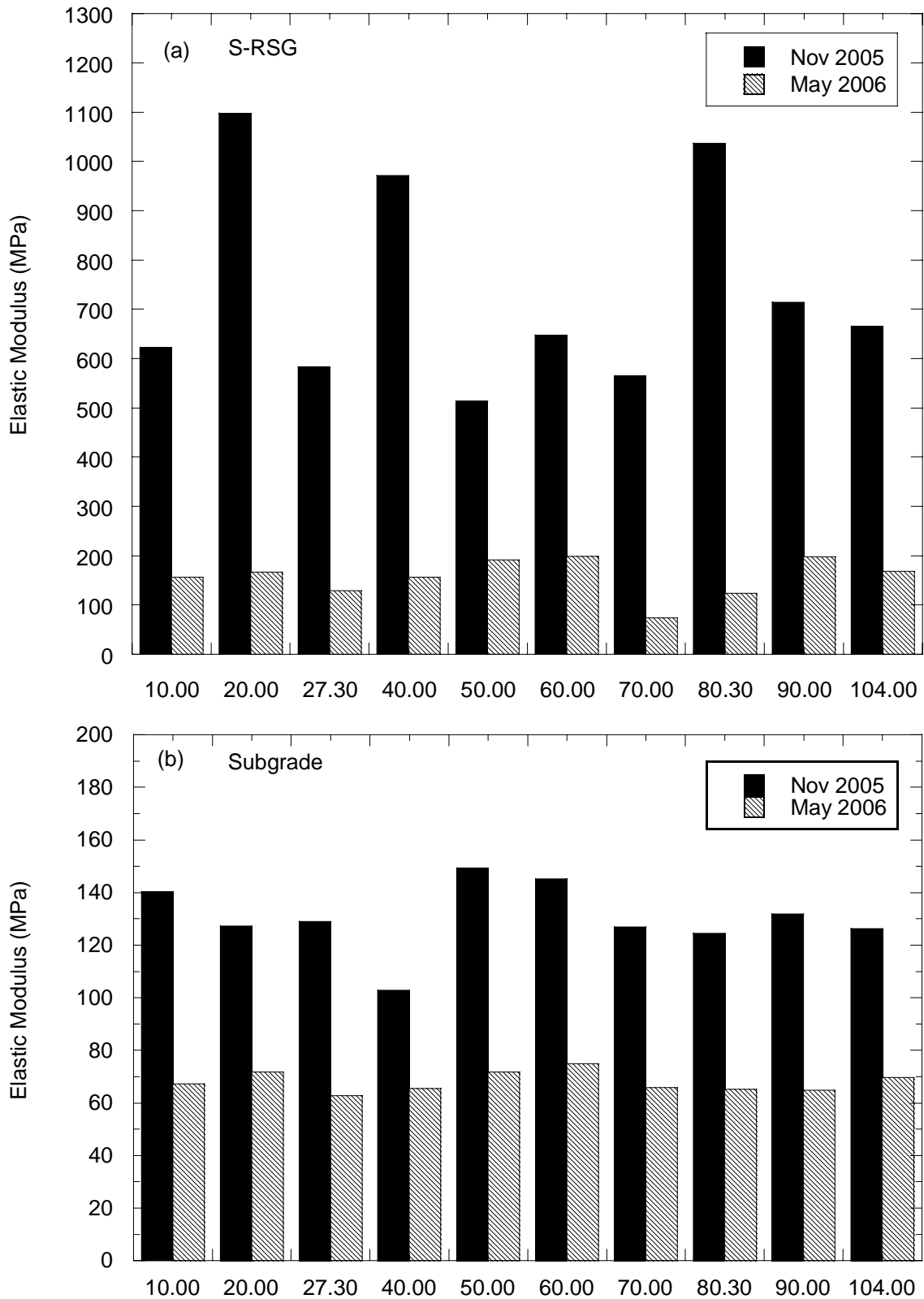
Fig. 26 Elastic moduli back-calculated from FWD tests by using MODULUS 6.0
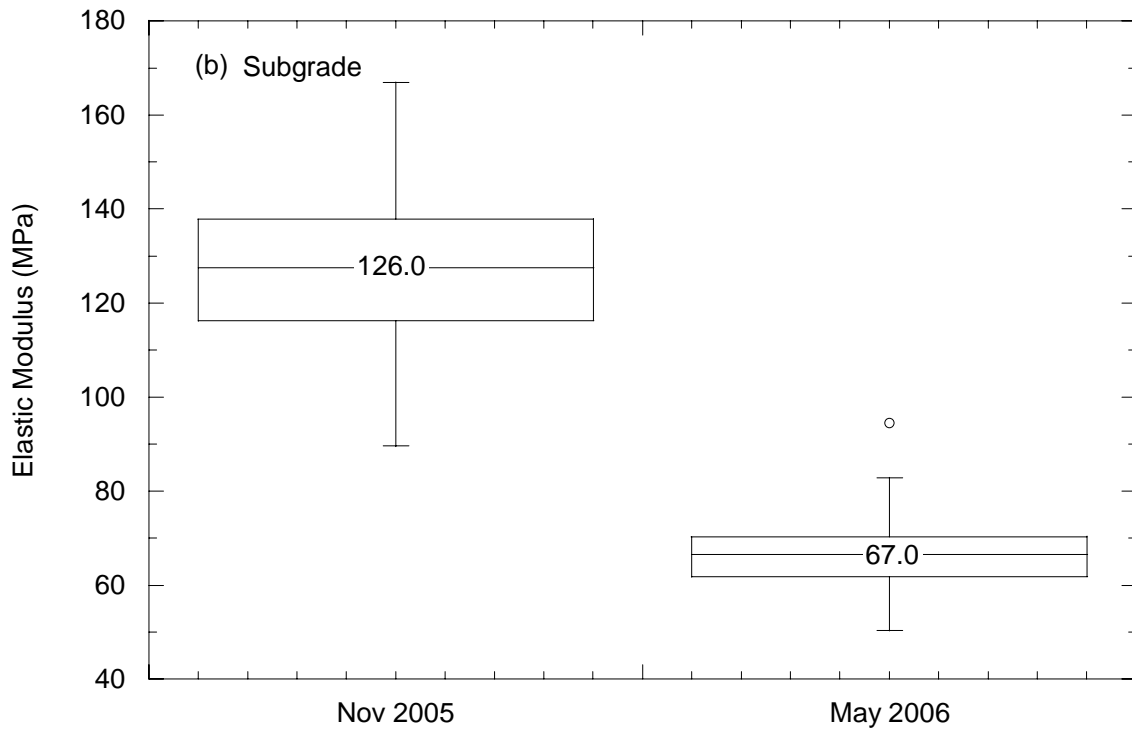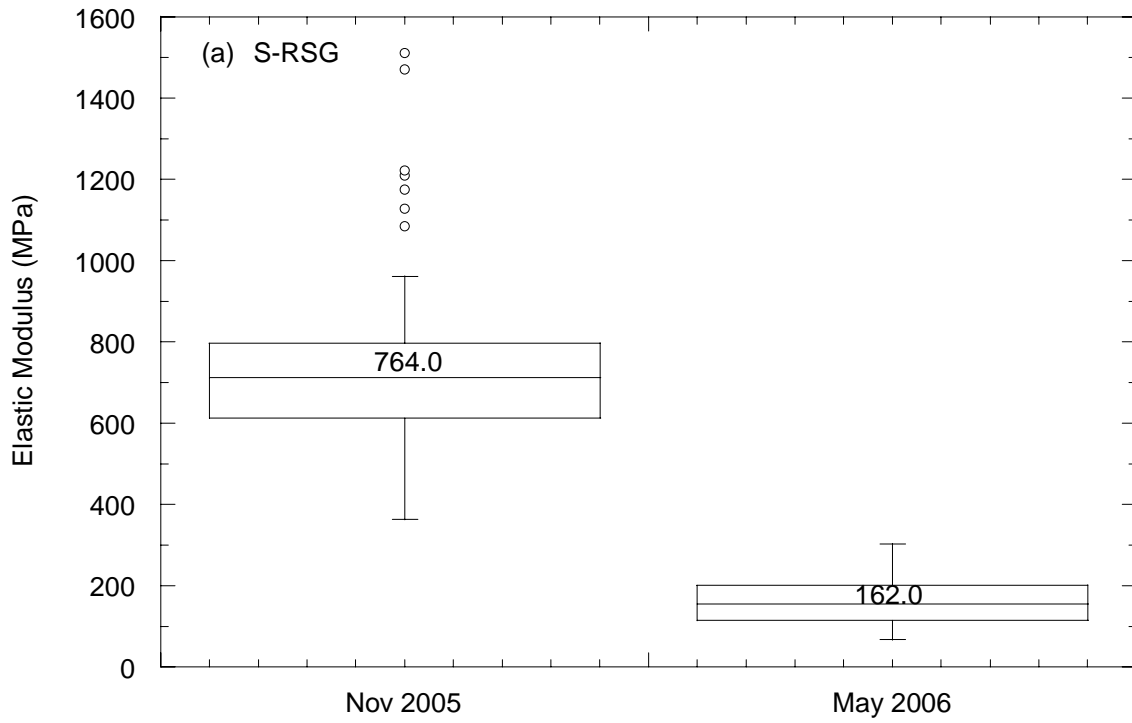software. (a) S-RSG (b) Subgrade.

Fig. 27 Statistical evaluation of Elastic moduli back-calculated from FWD tests by using MODULUS 6.0 software. (a) S-RSG (b) Subgrade.
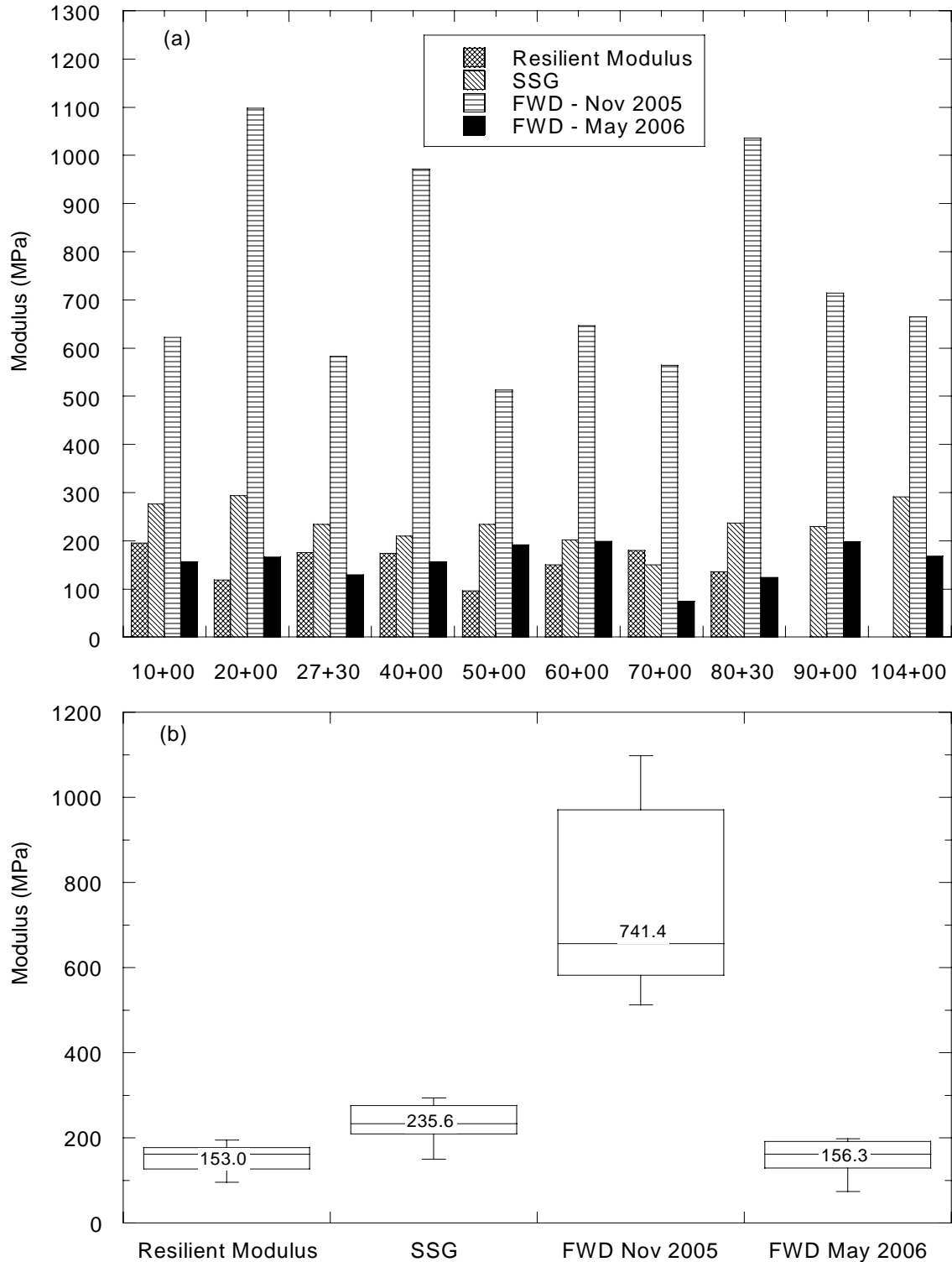
Fig. 28 Elastic modulus from laboratory resilient modulus, SSG and FWD tests (a) Modulus at each station (b) Statistical evaluation of results.